Bioorg. Med. Chem. 57 (2022) 116633

Contents lists available at ScienceDirect

Bioorganic & Medicinal Chemistry

journal homepage: www.elsevier.com/locate/bmc

Synthetic methodology-enabled discovery of a tunable indole template for COX-1 inhibition and anti-cancer activity

Gabriel Guerra Faura [a,1], Bocheng Wu [a,1], Adegboyega K. Oyelere [a,b,*], Stefan France [a,b,*]

[a] School of Chemistry and Biochemistry, Georgia Institute of Technology, Atlanta, GA 30332, United States
[b] Parker H. Petit Institute for Bioengineering and Bioscience, Georgia Institute of Technology, Atlanta, GA 30332, United States

A B S T R A C T

Establishing structure–activity relationships (SAR) for privileged pharmacophores, such as the indole scaffold, is a key step in the early stages of drug discovery. Herein, we report the synthesis and preliminary SAR studies on substituted 6-hydroxyindole-7-carboxylates as a tunable framework for COX inhibition and anti-cancer activity. To facilitate the SAR discovery, a modular synthetic methodology was employed which enabled the synthesis of the substituted indoles. From the synthesized compounds, five displayed COX-1 inhibition activity in a colorimetric assay with their intracellular activity further confirmed by a cell-based target validation assay. Following molecular docking analyses, key interactions between the active compounds and the COX enzymes were elucidated. In addition to the identified COX inhibitors, two compounds showed selective cytotoxicity against Hep-G2, MCF-7, and LnCaP. The mechanism of cell death was investigated and found to include induction of Caspase-3 activation and cleavage, down-regulation of anti-apoptotic proteins Bcl-xL and Bcl-2, and upregulation of Bax. Finally, two representative compounds were confirmed to induce cell cycle arrest at the G1/G0 stage. In summary, the 6-hydroxyindole-7-carboxylate framework shows promising versatility as a template for the discovery of anti-inflammation or anti-cancer agents, given the evidence of its COX inhibitory and anti-cancer activities herein presented.

1. Introduction

Structure-activity relationships (SAR) are central to the various stages of drug discovery, particularly during primary screening.[1] Establishing the existence of SAR for a particular system directly leads to strategic synthetic endeavors focused on obtaining more favorable physicochemical and biological properties. Often certain structural motifs offer interesting SAR across a range of biological systems. Such privileged structures serve as the starting point for elucidating novel mechanisms of action as well as identifying potential leads and can be readily accessed and derivatized through known synthetic approaches. One important example of a privileged structure is the indole framework (Figure 1). Indoles represent one of the most relevant classes of nitrogen heterocycles that are present in both naturally-occurring and synthetic compounds and have become very popular pharmacophores in drug discovery.[2,3] Indoles display a wide range of biological activities including, but not limited to, anticancer, antiviral, antifungal, anticonvulsant, and anti-inflammatory properties.

A variety of indole derivatives have been found to be active cyclooxygenase (COX) inhibitors.[4–8] COX enzymes are pro-inflammatory proteins, responsible for driving tissue inflammation and have been linked to tumorigenesis and cancer cell growth. In the human body, two COX isoforms can be present: COX-1, which is constitutively active in many tissues, especially in the gastrointestinal system (GI); and COX-2, which is generally expressed as a response to pro-inflammatory stimuli.[6] While expressed differently, both COX isoforms are associated with inflammatory response and have both been found to be overexpressed in a variety of cancers. As a result, COX inhibition has become a common biological target for the development of anti-inflammatory drugs as well as potential therapeutic agents for the treatment of cancer. Due to the success of Indomethacin, a marketed non-selective indole-containing COX inhibitor, the indole template represents a potential starting point for the identification of new COX inhibitors.

Toward this end, we sought to identify new indole-containing compounds that would offer selective COX isoform inhibition and/or interesting anti-proliferative activity against cancer cells. We previously disclosed a series of indomethacin-based COX-HDAC inhibitors that demonstrated potent and selective anti-cancer activities.[9] Furthermore, we reported a method that allows modular access to substituted 6-hydroxyindole-7-carboxylates via a Rh(II)-catalyzed benzannulation of α-diazo-β-ketoesters and enol ethers (Scheme 1).[10] Coupling this methodology with our ongoing interest in the identification of novel COX

Abbreviations: COX, cyclooxygenase; SAR, Structure-activity relationship; I3C, indole-3-carbinol; I3PA, indole-3-propionic acid; GI, gastrointestinal system.

* Corresponding authors.
E-mail addresses: aoyelere@gatech.edu (A.K. Oyelere), stefan.france@chemistry.gatech.edu (S. France).

[1] These authors contributed equally to the manuscript.

https://doi.org/10.1016/j.bmc.2022.116633
Received 1 November 2021; Received in revised form 10 January 2022; Accepted 20 January 2022
Available online 26 January 2022

enzymes-inhibiting scaffolds, we designed and synthesized indole derivatives that can serve as versatile templates for targeted SAR studies. Herein, we report the preparation of a small library of indole-containing analogues, which were separately profiled for their potential as COX inhibitors and anticancer agents.

2. Results and discussion

2.1. Compound synthesis

2.1.1. Synthesis of 6-hydroxy- and 6-methoxyindole-7-carboxylate derivatives 2 and 3.

Following our synthetic methodology,[10] α-diazo-β-ketoesters 1 were reacted with ethyl vinyl ether in the presence of $Rh_2(esp)_2$, bis[rhodium(α,α,α′,α′-tetramethyl-1,3-benzenedipropionic acid)], to afford indoles 2 (Scheme 2). Indoles 2 were subsequently treated with sodium hydride (NaH) in the presence of methyl iodide (MeI) to afford the corresponding 6-methoxy indoles 3 in good yields (Scheme 2).

2.1.2. Synthesis of C(7)-modified derivatives.

Interested in exploring modifications of the ester group, we hydrolyzed indole 3a with lithium hydroxide (LiOH) in 2,2,2-trifluoro (TFE) ethanol and water to afford the corresponding carboxylic acid 4. Upon 1-ethyl-3-(3-dimethylaminopropyl)carbodiimide (EDC)-mediated coupling with 2,2,2-trifluoroethylamine, amide 3d was obtained in 35% over the two steps (Scheme 3A). Ethyl ester 2e, on the other hand, was obtained in 20% yield through a direct transesterification of 3a in the presence of LiOH in ethanol (Scheme 3B).

2.1.3. Synthesis of C(3)-substituted derivatives.

To explore different substituents at the C(3) position, 3a was utilized as a starting point for the synthesis of several derivatives (Scheme 4). Acetylation of indole 3a with trifluoroacetic anhydride (TFAA) provided trifluoromethyl ketone 5, which was subsequently hydrolyzed with NaH in wet *N,N*-dimethylformamide (DMF) to afford carboxylic acid 6 in 83% over the two steps. Conversion of 6 into its corresponding acid chloride followed by coupling with aniline ($PhNH_2$) afforded the desired phenylamide 7 in 62% yield. Separately, alkylation of 3a with benzaldehyde followed by *in situ* reduction by triethylsilane (Et_3SiH) and trifluoroacetic acid (TFA) afforded benzyl-substituted indole 8 in 44% yield.

Since indole-3-carbinols (I3C) have shown anticancer and anti-inflammatory properties,[11] we sought to synthesize the I3C derivatives of indoles 2a, 3a and 3d, which was accomplished by a simple Vilsmeier-Haack formylation/reduction sequence to furnish compounds 10a-c (Scheme 5). Additionally, dimeric indoles 11a and 11b were prepared by treating 9b and 9c with lithium triethylborohydride ($LiEt_3BH$) followed by aqueous solution of ammonium chloride (NH_4Cl).

2.1.4. Synthesis of C(4)- and C(5)-substituted derivatives 12.

To probe the effects of substituents at the C(4)- and C(5)-positions of the indole, we synthesized derivatives 12 (Scheme 6). When diazo 1a was treated with 2-methoxystyrene or 1-ethoxypropene, the respective 4-phenyl- or 5-methyl-substituted indole 12a and 12b were obtained in 65% and 35% yield. Similarly, treatment of 1a with either 2-methylenetetrahydrofuran or dihydropyran provided 4- or 5-hydroxypropyl-substituted indoles 12c and 12d in 47% and 27% yield, respectively.

2.1.5. Synthesis of C(6)/C(7) regioisomeric indole 14.

As a direct comparison to 2a, the regiosiomeric indole 14 (the location of hydroxyl and carboxylate groups are switched at the C(6) and C(7) positions) was prepared in a two-step synthesis from α-diazo-β-ketoester 1a (Scheme 7). First, reaction with ethyl vinyl ether in the presence of $Cu(hfacac)_2$, copper(II) hexafluoroacetylacetonate, afforded dihydrofuran acetal 13 in 53% yield. Treatment of 13 with scandium(III) trifluoromethanesulfonate, $Sc(OTf)_3$, afforded the desired indole 14 in 18% yield.

2.2. COX inhibition study

2.2.1. Colorimetric inhibition screening

To probe the anti-inflammatory potential of the synthesized indoles, the compounds were tested for COX inhibition using a COX colorimetric inhibitor screening assay kit (Cayman #701050). Each compound was initially screened for both COX-1 and COX-2 inhibition activity at concentrations of 5 μM and 50 μM (Table 1). Celecoxib, a selective COX-2 inhibitor, and Indomethacin, a non-selective COX inhibitor, were utilized as positive controls.

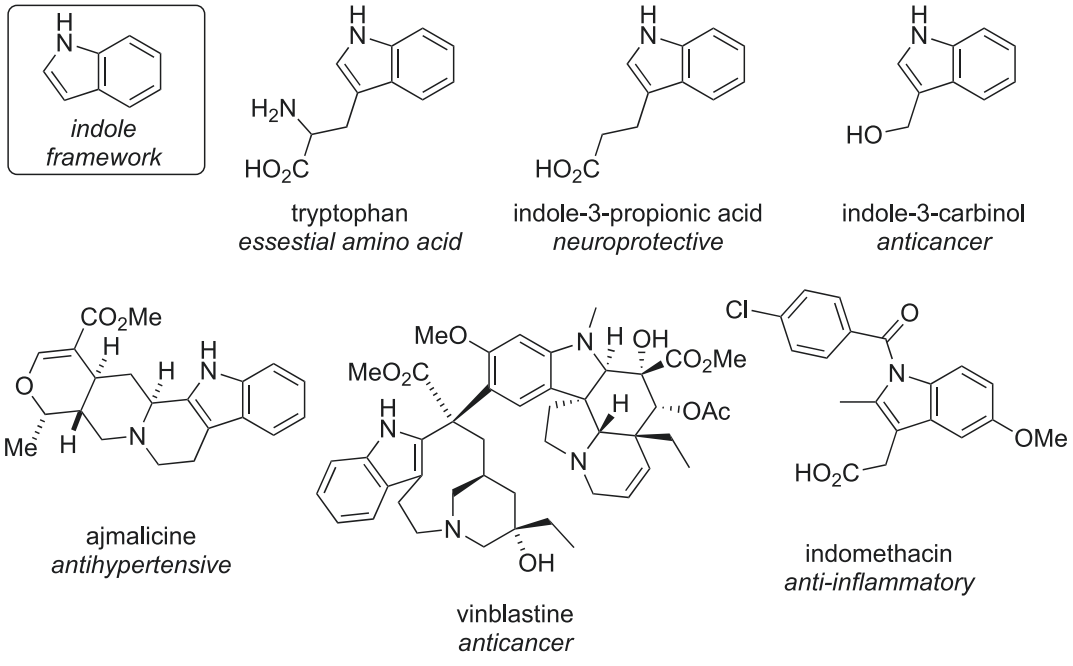

Figure 1. Indole and Representative Derivatives.

From the assay, we were pleased to identify compounds 2a, 2e, and 12b-d as COX-1 inhibitors and 10c as a COX-2 inhibitor, with inhibitory activities over 40% at the concentration of 50 μM. The assay also provided some initial SAR insights. For instance, the presence of a C(6)-hydroxy group in 2a seems to be crucial for COX-1 inhibition, as C(6)-methoxy derivative 3a was completely inactive against COX-1, while showing weak activity against COX-2. The C(3)-carbinol group seems to favor COX-2 inhibition, as seen in both 10b and 10c. Furthermore, as 10c had better activity against COX-2, it can be inferred that the amide at the C(7) position provides better binding to the COX-2 enzyme when compared to the ester at the C(7) position. Dimerization of these indoles and the swapping of the phenolic and trifluoroethyl ester moieties of 2a are detrimental to COX inhibition as compounds 11a-b and 14, respectively, are devoid of COX-1 and COX-2 inhibition activities. Interestingly, the identity of the substituents at positions C(4) and C(5) of 2a greatly influenced COX-1 inhibition. While compound 12a, an analogue of 2a with hydrophobic phenyl group at C(4)-position, lost the COX-1 inhibition activity seen in 2a, the introduction of sterically less hindered methyl or polar group at C(4) or C(5) is well tolerated as the resulting compounds 12b-d still elicit COX-1 inhibition.

To determine the IC_{50}s of the most active compounds and investigate their selectivity index for COX-1/2 inhibition, indoles 2a, 2e, 10c, 12b-d were screened at 8 different concentrations, ranging from 0.6 μM to 380 μM. Because they did not exhibit any significant COX inhibitory activity in the two-concentration assay (Table 1), compounds 3a (low activity) and 14 (inactive) were also tested as negative controls for the group. The representative dose–response curves of 2a, 2e, 3a, 10b, 12b-d (Figure S3) were then utilized to calculate the IC_{50}s and the COX-2/COX-1 selectivity index (SI) of the compounds (Table 2). All the other curves are shown in the Supporting Information.

Compound 2a showed moderate COX-1 inhibition ($IC_{50} = 12.6 \pm 2.5$ μM) with high selectivity over COX-2 ($SI > 30.2$). Similarly, 2e showed comparable COX-1 inhibition ($IC_{50} = 11.8 \pm 4.3$ μM) and $SI > 32.3$. Compounds 12b-d showed promising COX-1 inhibition, with 12d exhibiting an $IC_{50} = 5.6 \pm 1.2$ μM for COX-1 and weak COX-2 inhibition ($IC_{50} = 237.1 \pm 65$ μM). In agreement with the two-concentration assay, 10c selectively inhibited COX-2 ($IC_{50} = 8.65 \pm 3.0$ μM) with COX-2/COX-1SI = 0.1. Finally, as expected, 3a and 14 did not show any significant COX inhibition activity.

2.2.2. Cell target validation assay

While the initial cell-free assays were crucial to identify candidates with COX inhibition activity and estimate their respective IC_{50}, we are cognizant that small molecules may act differently in a cellular environment. Thus, to confirm the COX enzymes as the intracellular target, we sought to probe the activity of our compounds in a cell-based assay by utilizing a Prostaglandin E_2 (PGE_2) ELISA kit. Since PGE_2 is a product derived from COX activity, COX inhibition can be correlated to changes in the PGE_2 level expression, as inhibition of COX will lower PGE_2 levels.

Based on the colorimetric inhibition assay, compounds 2a, 2e, 10c, and 12b-d were selected for the cell-based assay, alongside with Celecoxib and Indomethacin as positive controls, and 3a and dimethylsulfoxide (DMSO) as negative controls. Although we were not able to determine its COX activity through the colorimetric assay, we were curious to test compound 10b due to its structural similarity to 10c, which was active against COX-2. Briefly, HeLa cells were treated with the corresponding compounds for 24 h; the cell culture media was then collected and centrifuged. Next, the supernatants were collected and analyzed using a PGE_2 ELISA kit to determine the PGE_2 levels (Figure 2).

The compounds with COX-1 inhibition activity, 2a, 2e, and 12b-d, showed significant downregulation of PGE_2 levels, with >40% and 80% inhibition at 50 μM and 100 μM respectively (Figure 2). Thus, through the ELISA assay, we confirmed that indoles 2a, 2e, and 12b-d inhibit COX enzymes intracellularly. As anticipated, compound 3a, which was not active against COX through the cell-free colorimetric assay, did not show any PGE_2 downregulation at 50 μM and 100 μM.

Relative to the COX-1 inhibitors, the effects of 10b and 10c on COX activity were rather unexpected. While 10c showed COX-2 inhibition in the colorimetric assay (Table 2), its activity was not strongly confirmed by the cell-based assay (Figure 2). Instead of a decrease in PGE_2 levels, we observed that, relative to the control, 10b and 10c caused an increase in PGE_2 levels in HeLa cells at 50 μM. This increase in PGE_2 levels was even more pronounced in the cells treated with 10b at 50 μM (Figure 2). However, when the cells were treated with 10b and 10c at 100 μM, the PGE_2 production was back to the same levels of the control. We believe that the relative increase in PGE_2 production could be due to a pro-survival response,[12–14] which was later counteracted by the use of a higher dose of 10b and 10c (100 μM).

2.2.3. Molecular docking Studies.

To gain better insight on how the tested compounds could bind to the COX enzymes and to evaluate their binding affinities, we performed virtual screenings on the lead candidates utilizing Autodock Vina 4.2. R.[15] For this docking study, we chose crystal structures solved with Celecoxib bonded to COX-1 protein (PDB: 3KK6) and COX-2 (PDB: 3LN1) to ensure uniformity when comparing the orientations adopted by our compounds at the binding sites of both enzymes relative to Celecoxib. Our docking outputs were evaluated using a combination of interaction energy (docking score) and geometrical matching quality, which is a more realistic evaluation of binding.[16] We first validated our docking protocol through the re-docking of Celecoxib to the active sites of both enzymes. We observed that Celecoxib adopted docked orientations that were identical to the ones in the crystal structures of both enzymes (Figure S4i).

Subsequent molecular docking on our lead compounds revealed differences among them, and also relative to Celecoxib, that may explain their COX-inhibition potency and selectivity. As seen in Figures 3A and 4A, our compounds bind in hydrophobic regions within COX-1 and COX-2 active pockets that are the same crystallographically validated binding sites for Celecoxib (note that the hydrophobic regions are depicted in a gradient red mesh). Based on the docked orientations, compounds 2a, 2e and 12d fit the binding pocket of the COX-1 protein better than 10b and 10c. Specifically, the interactions between their C(6)-hydroxyl and C(7)-ester groups and COX-1 Tyr-355′s phenol group is crucial to binding of

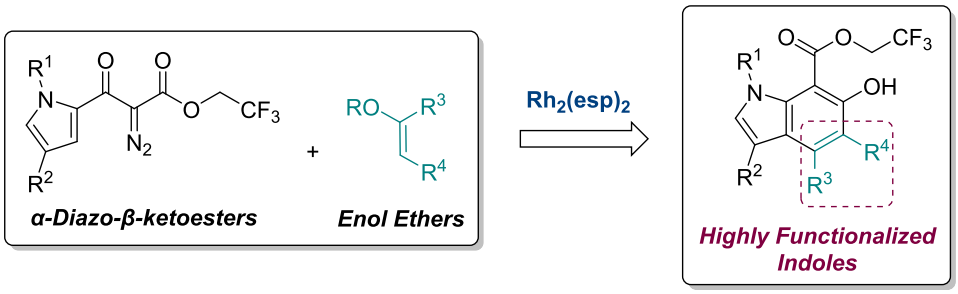

Scheme 1. Rh(II)-catalyzed Synthesis of 6-Hydroxyindole-7-carboxylates.

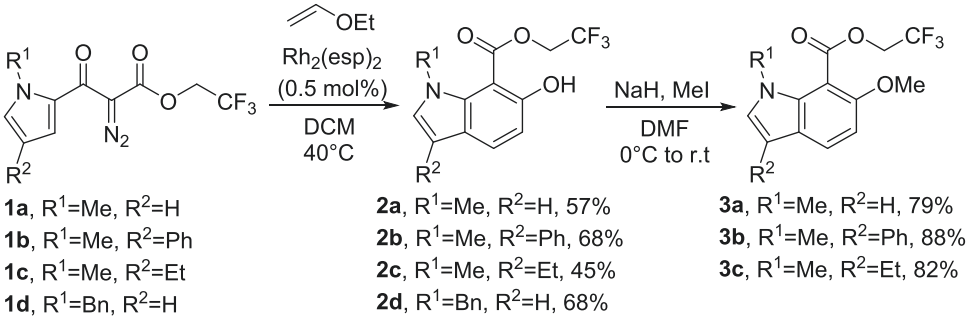

Scheme 2. Synthesis of indoles 2 and the corresponding 6-methoxy derivatives 3.

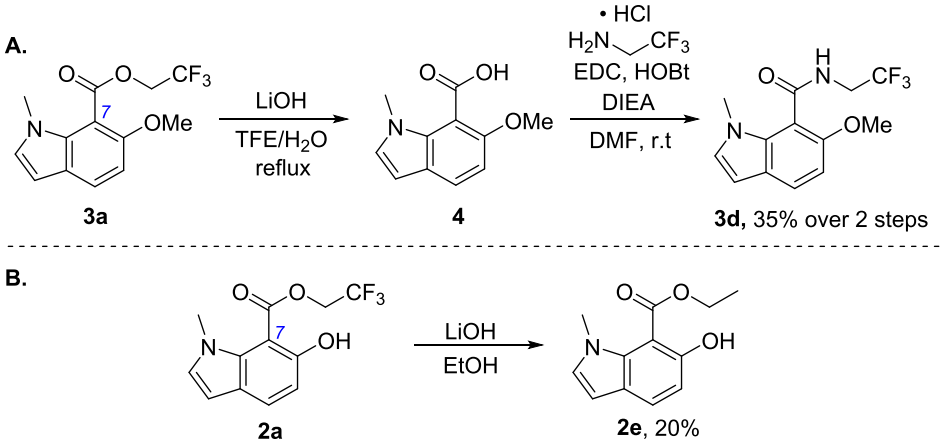

Scheme 3. Syntheses of amide 3d (A) and ethyl ester 2e (B).

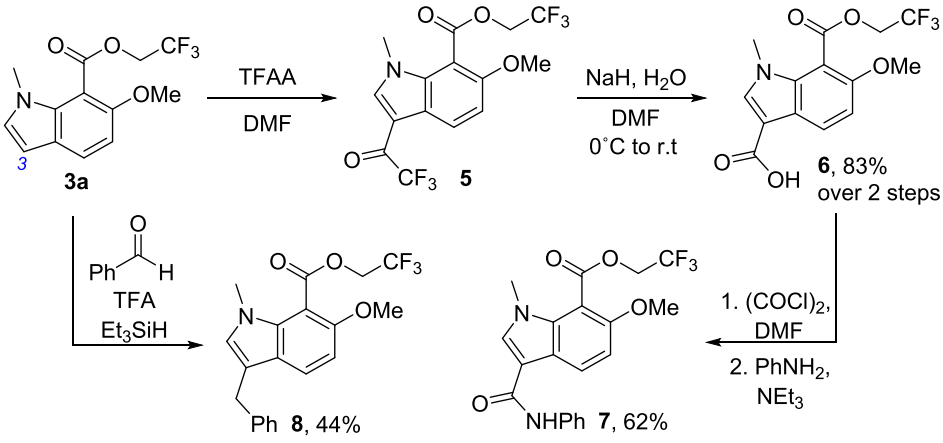

Scheme 4. Synthesis of C(3)-substituted indoles 6, 7 and 8.

2a and 2e to COX-1. This interaction is potentially further augmented by H-bonding between Arg-120 and the C(7)-ester group (Figures 3B-I-II). For compound 12d, the C(5) 1-hydroxypropyl arm reaches into a hydrophilic region in the vicinity of His-90 where it could potentially engage in H-bonding interactions with Ser-353, Leu-352, His-90, and Ser-516 (Figure 3B-III). Additionally, the trifluoro groups of 2a, 2e, 12d, and Celecoxib point to the region of Val-116, which is a relatively hydrophobic area (Figures 3B-I-III, VI). In contrast, compounds 10b and 10c adopted docked poses that are flipped 180° relative to those of 2a, 2e, 12d, and Celecoxib, with their C(3)-carbinol OH-groups forming bifurcated H-bonding with the carbonyls of Ser-353 and Leu-352. However, the orientations adopted by 10b and 10c placed their methoxy groups within a relatively hydrophilic area of the COX-1 active site, a scenario that may negatively impact binding affinity (Figure 3B-IV-V). Mofezolac, a control COX-1 selective inhibitor, also fits very well within COX-1 active site with its two p-methoxyphenyl moieties reaching to hydrophobic regions guarded by Phe-518/Trp-387 and Leu-345, while its carboxylic acid group forms strong electrostatic and H-bonding interactions with Arg-120 and Tyr-355, respectively (Figure S4ii-A).

Based on binding orientations, Celecoxib, 10b and 10c fit better into COX-2 active site compared to 2a, 2e, 12d and Mofezolac (Figures 4A,

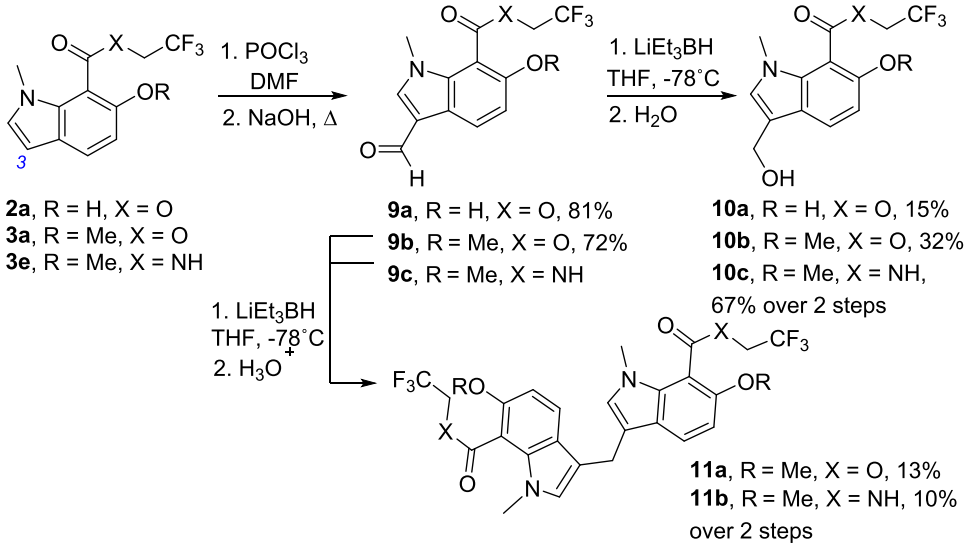

Scheme 5. Synthesis of I3C derivatives 10 and dimers 11.

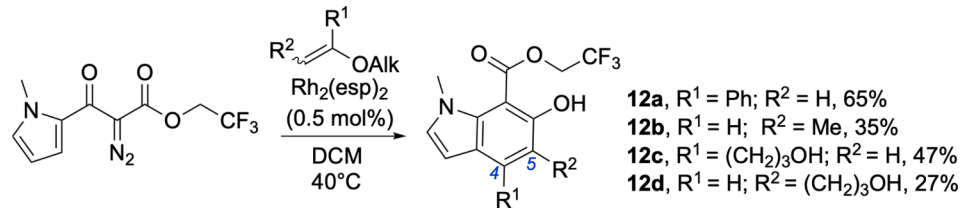

Scheme 6. Synthesis of C(4)- and C(5)-substituted derivatives 12.

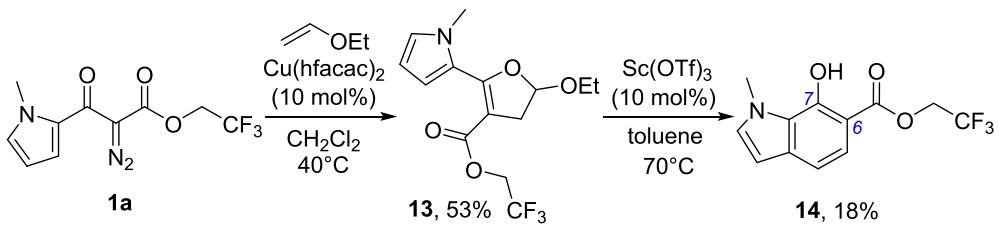

Scheme 7. Synthesis of C(6)/C(7)-regioisomeric indole 14.

4B and Figure S4ii-B). Specifically, the C(6)-methoxy groups of 10b and 10c are oriented toward hydrophobic area of Val-102, Val-335 and Leu-338, while their trifluoro groups are similarly pointed to hydrophobic region guarded by Phe-504, Trp-373, and Phe-367. Moreover, the C(3)-carbinol OH-groups of 10b and 10c are accommodated within an hydrophilic area where it could be stabilized via potential H-bonding with His-75 imidazole ring hydrogen and the carbonyl of Ser-339 (Figures 4B-I-II). The sulfonamide moiety of Celecoxib is similarly oriented to make stabilizing H-bonding interactions with His-75, Ser-339, Gln-178 and Arg-499. The Celecoxib trifluoro and toluyl groups are oriented toward the hydrophobic regions surrounded by Phe-504, Trp-373, and Phe-367; and Val-102, Val-335 and Leu-338, respectively (Figure 4B-III). Overall, this orientation allowed optimal binding of Celecoxib within COX-2 active site. In contrast, 2a, 2e and 12d are accommodated within the COX-2 binding site with somewhat weak stabilizing interactions. For 2a, His-75 and Ser-339, the closest amino acids whose side chains could potentially form H-bonding with the phenolic group of 2a, are 4.7 Å and 4.2 Å away, respectively, from this group (Figure 4B-IV). Although the phenolic groups of 2e and 12d are within 3.0 Å of Tyr-341 and carbonyl of Leu-338, respectively, the approximately 90° orientation makes the potential H-bonding interaction between these groups to be a weak one (Figure 4B-V-VI). [17] While the OH-group of the hydroxypropyl moiety of 12d is positioned for H-bonding with His-75 or Arg-299, this interaction could be off-set by potential steric clash between its trifluoro group and Phe-504.

The binding affinities obtained from the docking of these compounds further support the COX-2 selectivity of Celecoxib (COX-2, −11.9 kcal/mol vs COX-1, −7.9 kcal/mol) and 10c (COX-2, −8.1 kcal/mol vs COX-1, −7.0 kcal/mol); and COX-1 selectivity of Mofezolac (COX-1, −8.6 kcal/mol vs COX-2, −6.8 kcal/mol) and 12d (COX-1, −7.9 kcal/mol vs COX-2, −6.7 kcal/mol). Despite the experimental evidence of COX-1 selectivity (Table 2) and better accommodation at COX-1 active sites, the COX-1 and COX-2 docking scores of 2a (COX-1, −7.8 kcal/mol vs COX-2, −7.5 kcal/mol) and 2e (COX-1, −7.0 kcal/mol vs COX-2, −7.5 kcal/mol) are too close to strongly support selectivity for either enzyme.

2.3. *MTS assay for anti-proliferation studies in cancer cells.*

Following our COX inhibition activity investigations, the effect of the

Table 1
COX-1/2 inhibition activity of representative compounds.

Compound	COX-1 (5 μM) Inhibitory %	COX-1 (50 μM) Inhibitory %	COX-2 (5 μM) Inhibitory %	COX-2 (50 μM) Inhibitory %
2a	21.2 ± 0.1	57.3 ± 0.7	NI	NI
2b	[a]NI	23.0 ± 2.6	NI	NI
2c	NI	27.2 ± 1.8	NI	NI
2d	NI	[b]ND	NI	ND
2e	NI	46.92 ± 0.1	NI	NI
3a	NI	NI	NI	24.3 ± 7.3
3b	NI	NI	NI	NI
3c	NI	NI	NI	NI
3d	NI	NI	NI	NI
6	NI	NI	NI	NI
7	NI	NI	NI	NI
8	NI	NI	NI	NI
10a	NI	NI	NI	NI
10b	NI	33.3 ± 1.1	24.3 ± 2.7	ND
10c	NI	NI	35.0 ± 3.27	66.8 ± 3.8
11a	NI	22.9 ± 1.4	NI	NI
11b	NI	NI	NI	NI
12a	NI	NI	NI	NI
12b	31.9 ± 7.3	75.8 ± 2.2	NI	NI
12c	NI	59.0 ± 0.2	NI	NI
12d	32.7 ± 0.8	70.2 ± 1.3	NI	25.0 ± 4.5
14	NI	NI	NI	NI
Celecoxib	NI	21.4 ± 4	94.0 ± 0.6	95.8 ± 0.1
Indomethacin	66.5 ± 1.8	[c]NT	60.4 ± 1.6	NT

[a] NI implies inhibition<20%; [b]ND indicates unable to determine inhibitory activity due to precipitate formation. [c]NT stands for not tested.

Table 2
IC_{50} (μM) of COX inhibition and COX-2/COX-1 selectivity index of tested compounds.

Compound	COX-1 (μM)	COX-2 (μM)	Selectivity index (COX-2/COX-1)
2a	12.59 ± 2.5	>380	>30.2
2e	11.8 ± 4.3	>380	>32.3
3a	154.2 ± 41.6	>380	>2.5
10c	85.8 ± 14.2	8.7 ± 3.0	0.1
12b	13.0 ± 3.9	187.5 ± 74.4	14.4
12c	35.5 ± 5.0	>380	>10.7
12d	5.7 ± 1.2	237.1 ± 65	42.3
14	>380	>380	n/a
Celecoxib	48.0	0.40	0.0083
Indomethacin	0.2	1.1	5.5

synthesized indole compounds on the viability of selected cancer cell lines was probed through an MTS assay (Table 3). We were particularly interested in evaluating 2a, 2e, and 12b-d as relatively few COX-1 selective inhibitors have been investigated for anticancer activity. The selected cancer cell lines were Hep-G2 (hepatocellular carcinoma cell line), A549 (lung adenocarcinoma cell line), MDA-MB-231 (triple negative breast cancer cell line), MCF-7 (ER + breast cancer cell), DU145 (prostate cancer cell line lacking androgen receptor, $LnCaP^{F876L}$ (prostate cancer cell line that overexpresses mutated androgen receptor), and HeLa (cervical cancer cell line). A normal cell line, VERO (Kidney epithelial cell), was used to gauge selective toxicity to tumor cells. Celecoxib was used as a positive control given its known effects on cell viability. [18–20] The assay involved seeding of the cells into 96-well plate overnight followed by treatment with various concentrations of selected candidates.

Following the MTS assays, we observed that 2a exhibited low cytotoxicity against most of the tested cell lines, with the exception of HeLa cells ($IC_{50} = 90.8 \pm 3.5$ μM). Compound 2e also showed weak effects on cell viability, as most cell lines were not affected up to the maximum tested concentration. While compounds 3a and 3b had similar effects to 2a on cell viability, C(3)-carboxylic acid 6 showed no inhibition. The C(3)-carbinol derivatives, 10a-10c, showed moderate to potent cytotoxicity against the tested cancer cell lines. Particularly, 10b was the most potent in the series towards Hep-G2 with $IC_{50} = 7.63 \pm 0.4$ μM, in addition to high anti-proliferation effects on $LnCaP^{F876L}$ ($IC_{50} = 16.4 \pm 2.6$ μM) and MCF-7 ($IC_{50} = 15.2 \pm 3.0$ μM) cells. The cytotoxicity exhibited by 10b against the tested cancer cell lines could explain its unexpected upregulation of PGE_2, observed in the ELISA assay (Figure 2). As literature suggests the anti-cancer properties of indole-3-carbinol and its derivatives could be attributed to their dimeric form DIM, [21] we investigated the effects of dimers 11a and 11b on cell viability. Interestingly, both dimers did not induce cytotoxicity to any tested cells up to 500 μM, indicating the cytotoxicity of 10b and 10c is likely not attributed to their dimeric form. Lastly, we evaluated the effects of C(4)/C(5)-substituted derivatives 12a-d, among which 12b-d were confirmed to be COX-1 inhibitors. While 12b-d did not elicit strong cytotoxic effects, indole 12a showed similar inhibitory pattern as 10b, but relatively less potent. Celecoxib also showed moderate cytotoxicity to all tested cell lines. In contrast to 10b and 12a, Celecoxib did not elicit any discernible cell line-dependent selective toxicity. Thus, while the compounds that showed COX-1 inhibition activity were not cytotoxic against the tested cancer cell lines, C(3)-carbinol derivatives showed interesting effects on cell viability.

2.4. Cell cytotoxicity mechanism study

Since the C(3)-carbinol derivative 10b showed selective activity toward Hep-G2, MCF-7, and $LnCaP^{F876L}$ in the cell viability assays, we were interested in probing its intracellular mechanism(s) of cell cytotoxicity by studying caspase 3 (coordinates the proteolytic processing of cellular structures), survival proteins Bax and Bcl-2 (ratio serves as a marker that determines cell susceptibility to apoptosis), anti-apoptosis protein Bcl-xL (highly expressed in cancers and differs from Bcl-2 in its mechanism of inducing apoptosis), and Androgen Receptor[22–23] (AR, commonly expressed in prostate cancer cells and a subset of hepatocellular carcinoma and breast cancer cells). Therefore, we performed immunoblots for caspase 3 cleavage, Bax/Bcl-2 ratio,[18] Bcl-xL regulation, and AR expression using the Hep-G2 cell line, using DMSO served as a negative control. Celecoxib was used as a positive control, given it has been shown to induce cancer cell death through activation of caspase 3 and suppression of Bax and Bcl-2. Furthermore, it has been shown that Celecoxib can also downregulate AR at mRNA and protein levels.[24]

Although the COX-1 selective inhibitors (2a, 2e, 12b-d) demonstrated weak activity in the cancer cell viability assay, we were still interested in learning more about their intracellular mechanism of cell cytotoxicity. We postulated that they may also induce cell death by a similar mechanism as Celecoxib, the positive control. Thus, 2a was selected as a representative COX inhibitor compound for the cytotoxicity study.

As anticipated based on literature reports,[25] Celecoxib caused caspase 3 cleavage while suppressing and Bcl-2 at its IC_{50} concentration (75 μM). Furthermore, Celecoxib showed Bcl-xL downregulation and Bax upregulation, increasing the Bax/Bcl-2 ratio which is expected to induce cell death. Compound 2a, which elicits a suppressive effect on PGE_2 production (Figure 2), shows cell apoptosis effects similar to Celecoxib near its IC_{50} (Figure 5). Compound 10b, which is most cytotoxic towards Hep-G2 among the disclosed indole compounds, also has a similar effect as Celecoxib at 20 μM with even more significant induction of cell death via caspase 3 cleavage and Bax/Bcl-2 ratio upregulation. It is likely that both novel indole compounds shared similar mechanisms of cell death as Celecoxib, such as ER stress and apoptosis.

Similar to the work of Pan et al., Celecoxib at 75 μM caused only a slight downregulation of AR expression, relative to the DMSO control after 24 h treatment, an effect that is within the limit of our statistical analysis.[26] We found that both 2a and 10b significantly downregulated AR expression, with 10b showing evidence of a dose-dependent effect (Figure 5). The AR downregulation effect caused by Celecoxib is largely

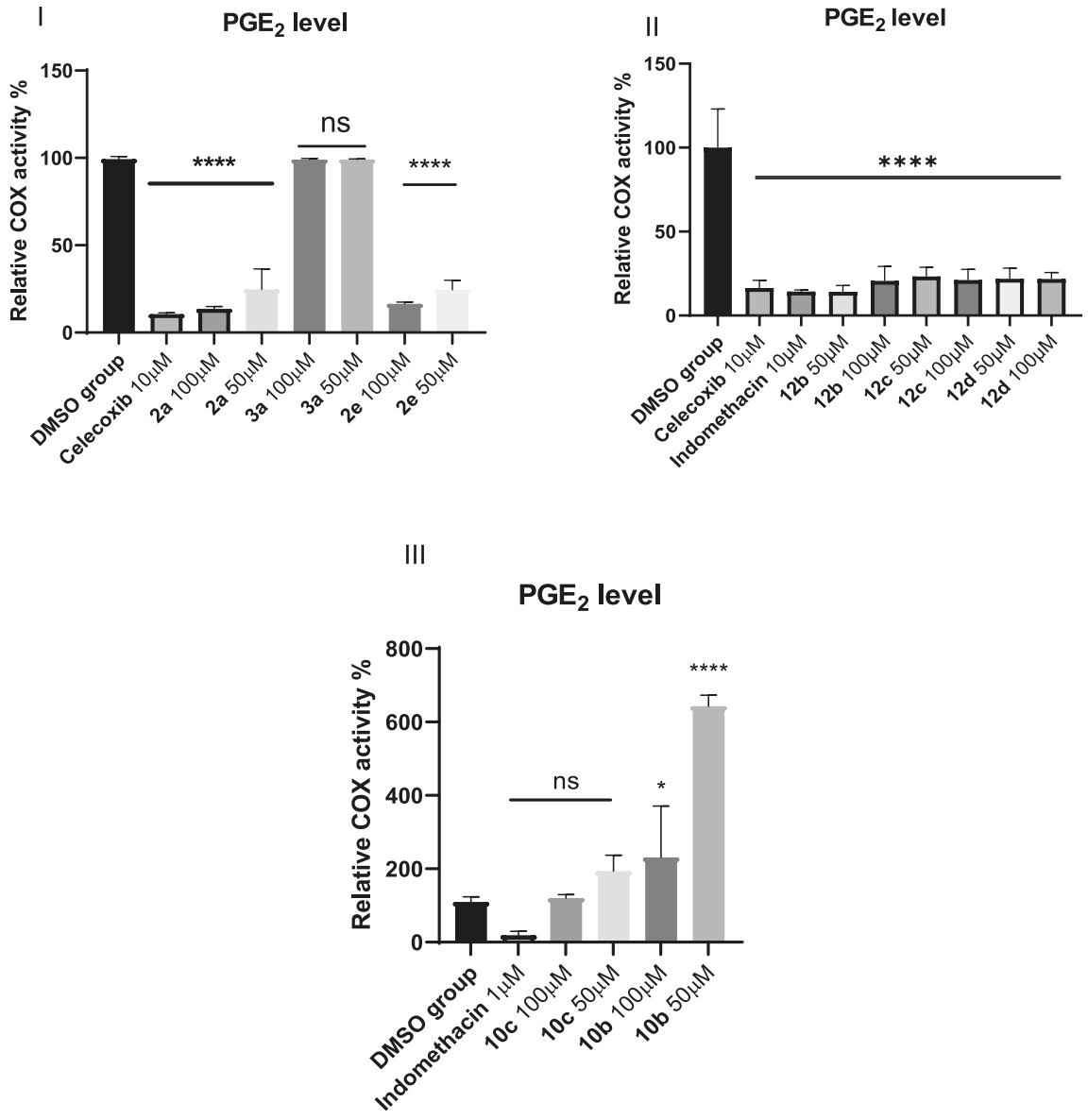

Figure 2. PGE_2 levels in HeLa cells treated with indole derivatives. Cells ($1*10^6$ count/well) were seeded to 6-well plate for 24 h prior to drug treatment. DMSO, or 0.1% DMSO solution of Celecoxib (10 μM), indomethacin (1 μM or 10 μM), 2a, 2e, 3a, 10b, 10c, 12b-d (50 and 100 μM) were added to the cells in 1 mL medium for 24 h. Data from two independent experiments performed in duplicate. Statistic bars show mean plus standard deviation; Statistic calculation was performed via Ordinary One-way ANOVA compare with control group, *P < 0.0332; **P < 0.0021; ***P < 0.0002; ****P < 0.0001, ns = not statistically significant).

mediated by EP2/CREB signaling.[24] It is possible that 2a acts through COX inhibition and EP2 signaling regulation in a similar manner as Celecoxib. However, additional unclear mechanisms may contribute to the cytotoxicity of 10b since it does not target COX.

2.5. Cell cycle arrest

Celecoxib has been shown to induce G1/G0 cell cycle arrest in Hep-G2 cells.[15] It is known to arrest cell cycle in G1 phase in many cancer cells due to mechanism(s) of cell death[27] that are unrelated to its COX-2 inhibition.[20] It is possible that our COX-1 and COX-2 inhibiting indoles are also causing COX-independent cell death. To investigate this prospect, we first tested 2a (as a representative COX-1 inhibitor) at 125 and 250 μM for 48 h (Figure S6-A) and 400 and 800 μM for 24 h (Figures 6 and S5) in a cell cycle assay using Hep-G2 cells and directly compared to Celecoxib at 100 μM. The concentrations of 2a that we chose for this experiment ranged from approx. 0.4x to 2.7x its IC_{50} against Hep-G2 cells (Table 3). The protocol for the cell cycle analysis was as we described in our previous work.[28] We observed that, like Celecoxib, indole 2a induced cell cycle arrest at the G1/G0 stage after 24 h and 48 h treatment, which could be the cause of the cell apoptosis that we observed in the data shown in Figure 5.

Next, we tested 10b in the cell cycle arrest assay. We observed that 10b at 12.5 and 25 μM for 48 h (Figure S6-B) and 25 and 50 μM for 24 h (Figures 6B and S5) induced G1/G0 stage cell cycle arrest as well. This result supports the postulation that 10b might cause cell apoptosis through G1/G0, similar to 2a, but possibly via COX-independent mechanisms.

3. Conclusion

Herein, we reported the synthesis of a small library of targeted indole derivatives alongside their preliminary biological data for COX inhibition and anti-cancer activity. The compounds were accessed through a

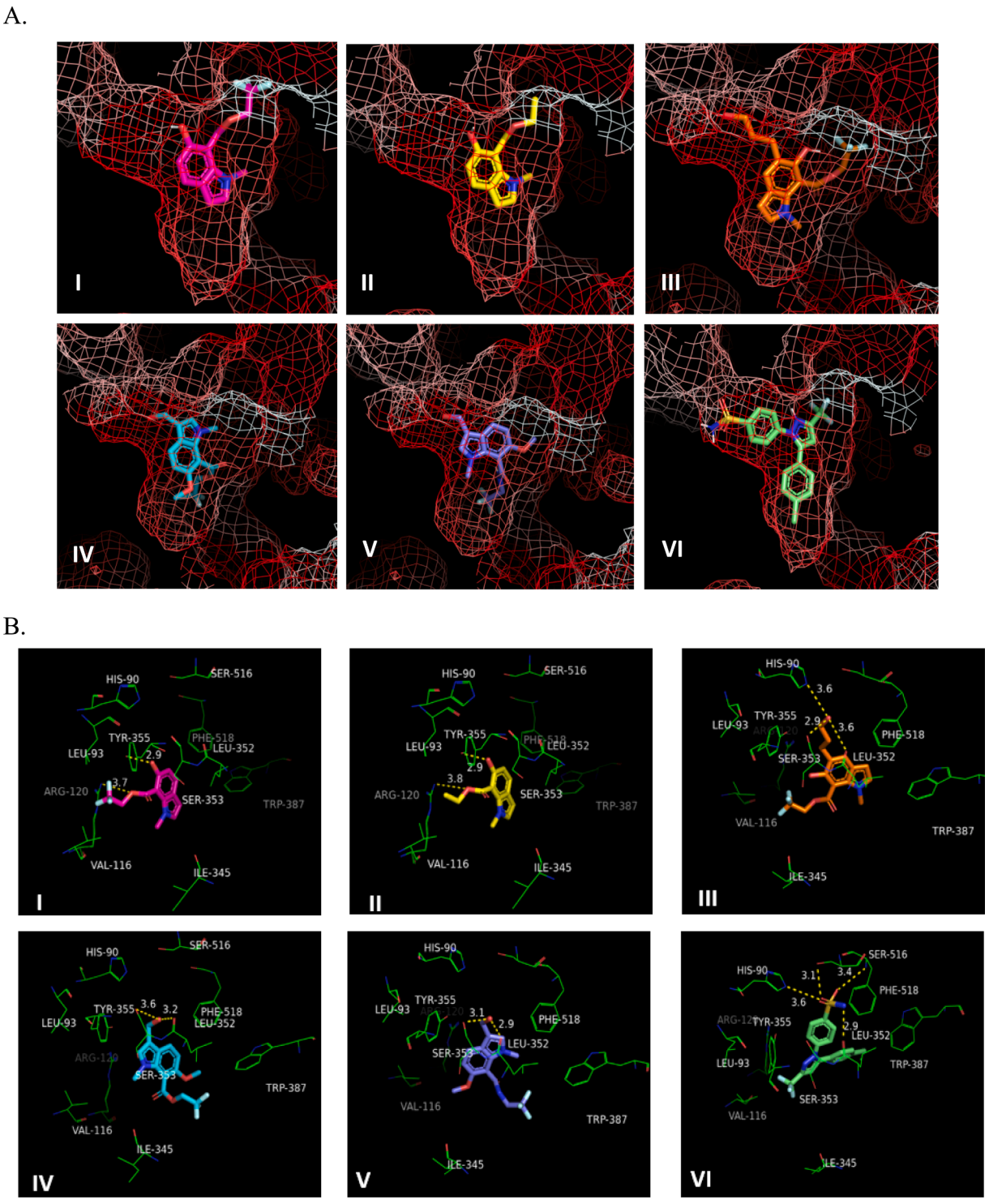

Figure 3. (A) Molecular docking analysis showing the interaction of 2a (A-I), 2e (A-II), and 12d (A-III), 10b (A-IV), 10c (A-V), celecoxib (A-VI) with the hydrophobic (in red) and hydrophilic (in white) regions of the COX-1 active pocket (PDB:3KK6); (B) Detailed H-bonding interactions of 2a (B-I), 2e (B-II), 12d (B-III), 10b (B-IV), 10c (B-V), celecoxib (B-VI).

modular Rh(II)-catalyzed reaction of 1-pyrrolyl α-diazo-β-ketoesters and enol ethers, followed by further derivatizations. This synthetic methodology offers tunable modification of the C(3)- to C(7)-positions of the indole scaffold.

COX inhibition data was collected by performing colorimetric assays, intracellular target validation, and computational docking investigation. Through these methods, we identified indoles 2a, 2e, 12b-d as selective COX-1 inhibitors. Also, 10c was shown to be COX-2 selective in a cell free assay although its on-target effect was not strongly confirmed in a cell-based assay. The key structural feature of indole 2a, 2e, 12b-d is the presence of a hydrogen at the indole C(3)-position. Similarly, changes to the ester C(6)-carboxyl group were tolerated, along with C(4)- and C(5)-substituents. These compounds could serve as templates for the discovery of more potent COX-1 inhibitors.

Similarly, anti-cancer effects were probed through MTS cell viability assays and cell death mechanism studies. Based on the MTS assay, the C

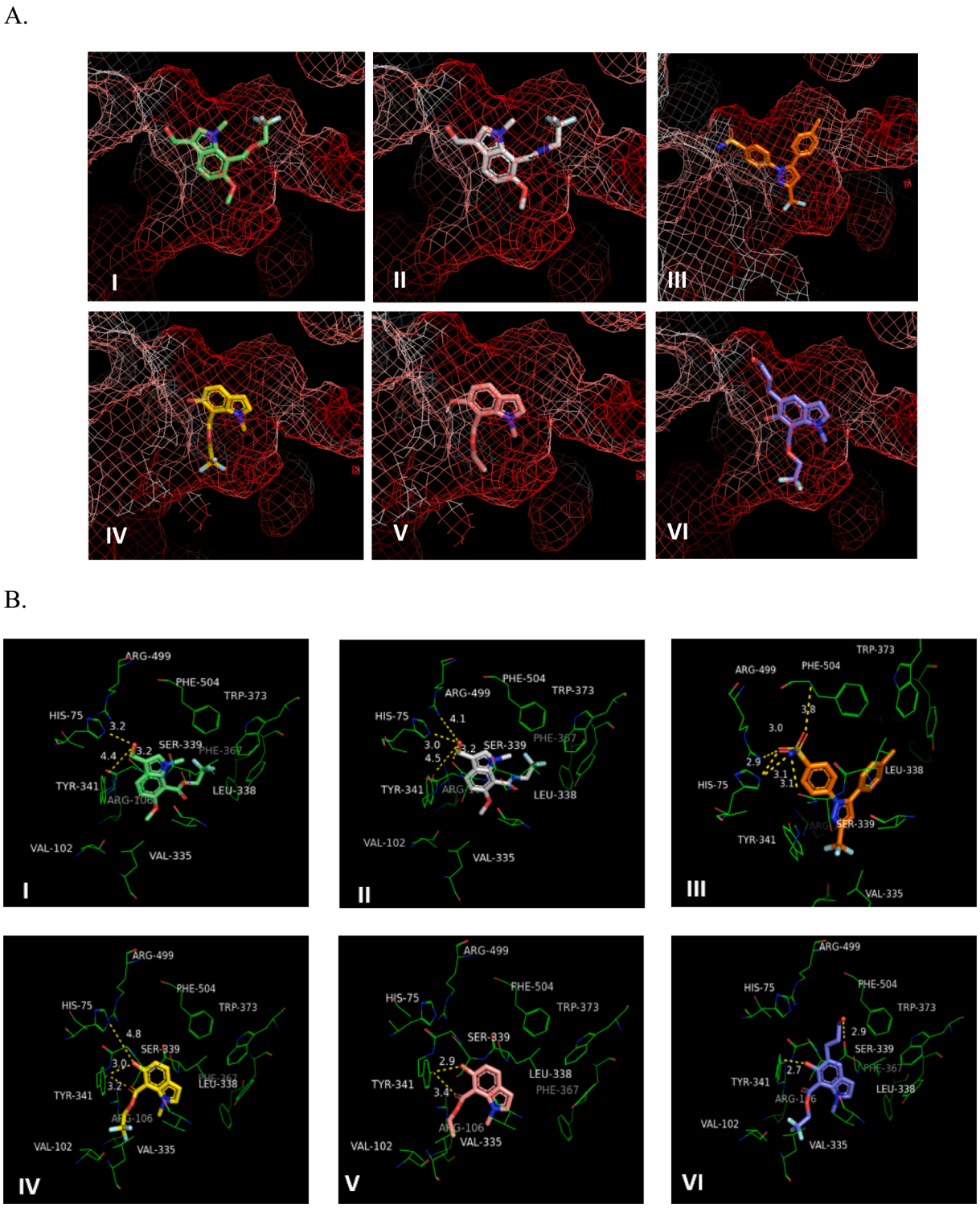

Figure 4. (A) Molecular docking analysis showing the interaction of 10b (A-I), 10c (A-II), Celecoxib (A-III), 2a (A-IV), 2e (A-V), 12d (A-VI). with the hydrophobic (in red) and hydrophilic (in white) regions of the COX-2 active pocket (PDB:3LN1); (B) Detailed H-bonding interactions of 10b (B-I), 10c (B-II), Celecoxib (B-III), 2a (B-IV), 2e (B-V), 12d (B-VI).

(3)-carbinol compounds 10b and 10c showed interesting cell-type selective cytotoxicity. Specifically, indole 10b was active against Hep-G2, MCF-7, and LnCaP^{F876L}, while demonstrating>20-fold selectivity for Hep-G2 when compared to VERO. Through investigating the mechanism of cell death, 2a and 10b were found to induce apoptosis via down-regulation of Bcl-2 families and AR, and upregulation of Bax, which is similar to Celecoxib. In addition, the compounds induce Hep-G2 cell cycle arrest at the G1/G0 stage which is also identical to Celecoxib. The AR downregulation effects of 2a and 10b could be due to their regulation of EP2/CREB signaling in analogous manner to that of Celecoxib. Given the selective cytotoxicity of 10b, more investigations are needed to understand the mechanistic basis of the anti-proliferative effects of 10b. Nevertheless, compound 10b and the overall 6-hydroxyindole-7-carboxylate template herein disclosed hold potential for the identification and

Table 3
Effects of representative indoles on cell viability as determined by MTS assay (all IC_{50}s are in μM).

	Hep-G2	A549	VERO	MDA-MB-231	MCF-7	DU145	LnCaP (F876L)	HeLa
2a	301.3 ± 13	419 ± 12	499.80 ± 2	355 ± 12	338 ± 16	277 ± 8	255 ± 23	90.8 ± 3.5
2e	483.7	NI	NI	NI	NI	NI	NI	NT
3a	280 ± 11	NI	NI	380 ± 17	276 ± 23	430 ± 6	139 ± 8	127.2 ± 6.8
3b	104.9	NI	NI	78.8	378	139	85.2	101.0 ± 21.0
6	NI	NI	NI	NI	NI	NI	NI	NI
10a	54.8 ± 1.7	219 ± 16	268 ± 33	NT	NT	NT	NT	NT
10b	7.63 ± 0.4	179 ± 5	198 ± 9	51.8 ± 8.7	15.20 ± 3.0	55.76 ± 3.2	16.39 ± 2.6	58.1 ± 8.5
10c	58.2 ± 5.0	163.6 ± 19	228.6 ± 26.2	252.7 ± 23.3	273.4 ± 14.7	144.1 ± 16.5	98.97 ± 5.5	110.1 ± 7.2
11a	NI	NI	NI	NI	NI	NI	NI	NT
11b	NI	NI	NI	NI	NI	NT	NT	NT
12a	58.9	206.2	140.1	138.5	56.3	122.3	47.6	NT
12b	183.1	468.8	413.7	338.8	194.7	390.6	180.1	>100
12c	385.3	NI	NI	NI	NI	NI	209.3	>100
12d	192.4	463.9	NI	363.0	203.2	394.3	117.3	>100
Celecoxib	58.20 ± 1.9	57.87 ± 3.3	60.63 ± 6.3	69.64 ± 10.0	64.19 ± 5.8	59.34 ± 4.0	16.40 ± 3.8	58.20 ± 1.9

NI: no inhibition up to 500 μM; NT: not tested.

development of novel COX inhibitors and new class of chemotherapeutic agents for the treatment of HCC, prostate cancer or breast cancer. The tunability of the synthetic methodology that furnished this densely functionalized indole carboxylates is crucial for a facile access to this class of compound in support of SAR studies essential to establish their therapeutic potential.

4. Experimental

4.1. Chemistry

4.1.1. General Information

Chromatographic purification was performed as flash chromatography with Silicycle SiliaFlash P60 silica gel (40–63 μm) or preparative thin-layer chromatography (prep-TLC) using silica gel F254 (1000 μm) plates and solvents indicated as eluent with 0.1–0.5 bar pressure. For quantitative flash chromatography, technical grades solvents were utilized. For purposes of accessing samples for screening, isolated yields were unoptimized for compounds not previously reported. Analytical thin-layer chromatography (TLC) was performed on Silicycle SiliaPlate TLC silica gel F254 (250 μm) TLC glass plates. Visualization was accomplished with UV light. Infrared (IR) spectra were obtained via attenuated total reflection (ATR) with a diamond plate using a Bruker ALPHA Fourier-transform infrared spectrophotometer. The IR bands are characterized as broad (br), weak (w), medium (m), and strong (s). Proton and carbon nuclear magnetic resonance spectra ^{1}H NMR and ^{13}C NMR) were recorded on a Varian Mercury Vx 300 MHz spectrometer or a Bruker 500 MHz spectrometer with solvent resonances as the internal standard ^{1}H NMR: $CDCl_3$ at 7.26 ppm or DMSO-d_6 at 2.50,^{13}C NMR: $CDCl_3$ at 77.0 ppm or DMSO-d_6 at 39.5). ^{1}H NMR data are reported as follows: chemical shift (δ, ppm), multiplicity (s = singlet, d = doublet, dd = doublet of doublets, dt = doublet of triplets, ddd = doublet of doublet of doublets, t = triplet, m = multiplet, br = broad), coupling constants (Hz), and integration. Mass spectra were obtained through EI on a Micromass AutoSpec machine or through ESI on a Thermo Orbitrap XL. The accurate mass analyses run in EI mode were at a mass resolution of 10,000 and were calibrated using PFK (perfluorokerosene) as an internal standard. The accurate mass analyses run in EI mode were at a mass resolution of 30,000 using the calibration mixture supplied by Thermo. HPLC analysis, which showed the compounds to be at least 95% pure, was performed on an Agilent 1260 HPLC with a Phenomenex C18 reversed phase HPLC column (100 × 4.6 mm) at a flow rate of 0.5 mL/min; using 0.1% v/v formic acid in H_2O (solvent A) and 0.1% v/v formic acid in MeCN (solvent B). The solvent gradient for chromatography elution is as follows: 5% solvent B from 0 to 5 min, linear gradient to 100% solvent B from 5 to 31 min, linear gradient to 5% solvent B from 31 to 33 min, 95% solvent B from 33 to 35 min, linear gradient to 5% solvent B from 36 to 38 min, 95% solvent B from 38 to 40 min, linear gradient to 5% solvent B from 40 to 41 min.

4.1.2. General procedure for the ssynthesis of 6-hydroxy indoles (2a-2d and 12a-12d)

Following a reported literature procedure[10] to a flame-dried flask equipped with a magnetic stir, $Rh_2(esp)_2$ (0.5 mol%) is added followed by dry DCM (0.2 M) and corresponding enol ether (1.5 to 10 equiv.) under constant nitrogen flow. After attaching a reflux condenser and bringing the reaction mixture to a boil, a 0.2 M solution of diazo compound 1 in dry DCM is slowly added over 1 h via syringe pump. After all the contents are added, let mixture reflux for further 15 min or until all starting material has been consumed (indicated by TLC analysis). Remove reaction mixture from heat and add a scoop of silica gel 300–400 mesh and let it stir for an additional 0.5 h-2 h. The solvent is then removed under pressure and the crude silica dispersion is purified on silica gel supported column chromatography to afford indoles 2a-2d and 12a-d. HPLC analyses: 2a retention time = 31 min, 12b retention time = 34.4 min, 12c retention time = 28.3 min and 12d retention time = 30 min.

Ethyl 6-hydroxy-1-methyl-1*H*-indole-7-carboxylate (2e). To an ice-cold solution of 2a (48.9 mg, 0.178 mmol) in EtOH (1.8 mL, 0.1 M), NaH (36.6 mg, 0.915 mmol) was added. Upon completion, the mixture was quenched with addition of water, extracted with Et_2O (3 × 3 mL), dried over $MgSO_4$ and vacuum-filtered through a short silica plug to afford 2e as a clear oil (8.0 mg, 20% yield). ^{1}H NMR (500 MHz, $CDCl_3$) δ 10.50 (s, 1H), 7.66 (d, J = 8.5 Hz, 1H), 6.93 (d, J = 3.2 Hz, 1H), 6.80 (d, J = 8.5 Hz, 1H), 6.49 (d, J = 3.2 Hz, 1H), 4.54 (q, J = 7.1 Hz, 2H), 3.80 (s, 4H), 1.48 (t, J = 7.2 Hz, 4H). ^{13}C NMR (126 MHz, $CDCl_3$) δ 169.6, 159.2, 134.3, 130.4, 128.3, 123.8, 110.4, 102.7, 98.9, 61.4, 38.4, 14.3. HRMS (ESI) *m/z*: $[M + H]^+$ Calcd for $C_{12}H_{13}NO_3$ 220.0968, found 220.0968. Retention time = 30.5 min

4.1.3. General procedure for the synthesis of 6-methoxy indoles (3a-3d)

To an ice-cold solution of the corresponding indole (1 equiv.) in dry DMF (0.1 – 0.2 M), NaH (60% dispersion in mineral oil, 1.5 equiv.) was added and the reaction was kept at the same temperature for 30 min. Methyl iodide (3.0 equiv.) was then added to the reaction mixture and the reaction and the ice-bath is removed. Upon complete disappearance of the starting material (monitored through TLC analysis), the reaction was cooled to 0 °C, quenched with water, extracted with EtOAc (3x) and dried over $MgSO_4$. Upon vacuum filtration through a Celite plug, the reaction mixture was concentrated under reduced pressure and the crude material was purified through silica-gel column chromatography to afford the desired 6-methoxy indoles.

2,2,2-Trifluoroethyl 6-methoxy-1-methyl-1*H*-indole-7-carboxylate (3a). Prepared by following the general procedure using indole 2a

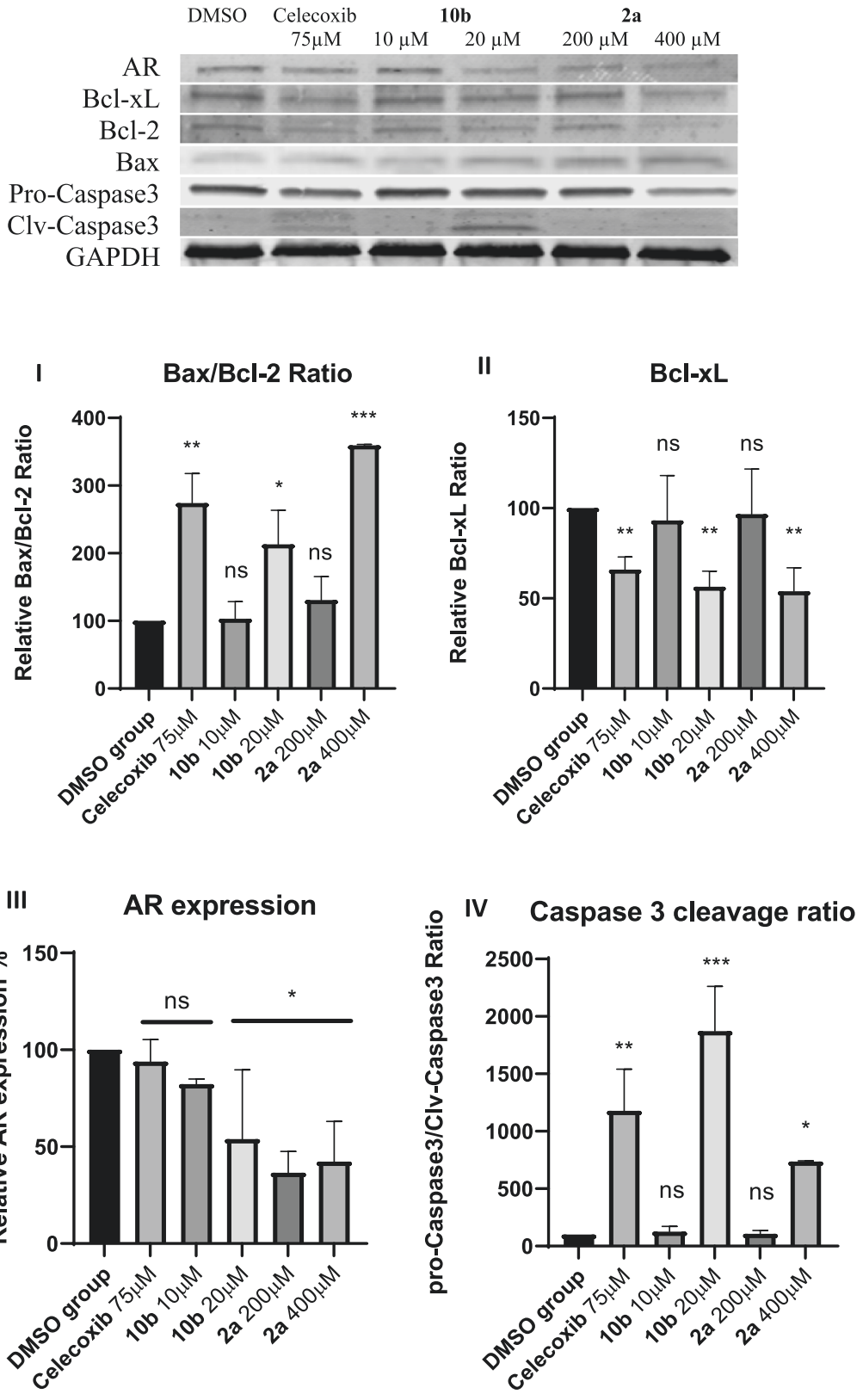

Figure 5. Western blot data showing the effects of 2a and 10b on apoptosis signaling in Hep-G2 cells. (A) Cropped gels showing the status of the target proteins after treatment with DMSO or DMSO solution of Celecoxib (75 μM), 10b (10 and 20 μM), 2a (200 and 400 μM). Cells were treated for 20 h. Note that the tested concentrations for 2a and 10b are approximately IC_{50}s or 2x IC_{50}. (B) Quantification of the cropped gels. Statistic bars show mean plus standard deviation; Statistic calculation was performed via Ordinary One-way ANOVA compare with control group, *P < 0.0332; **P < 0.0021; ***P < 0.0002; ****P < 0.0001, ns = not statistically significant).

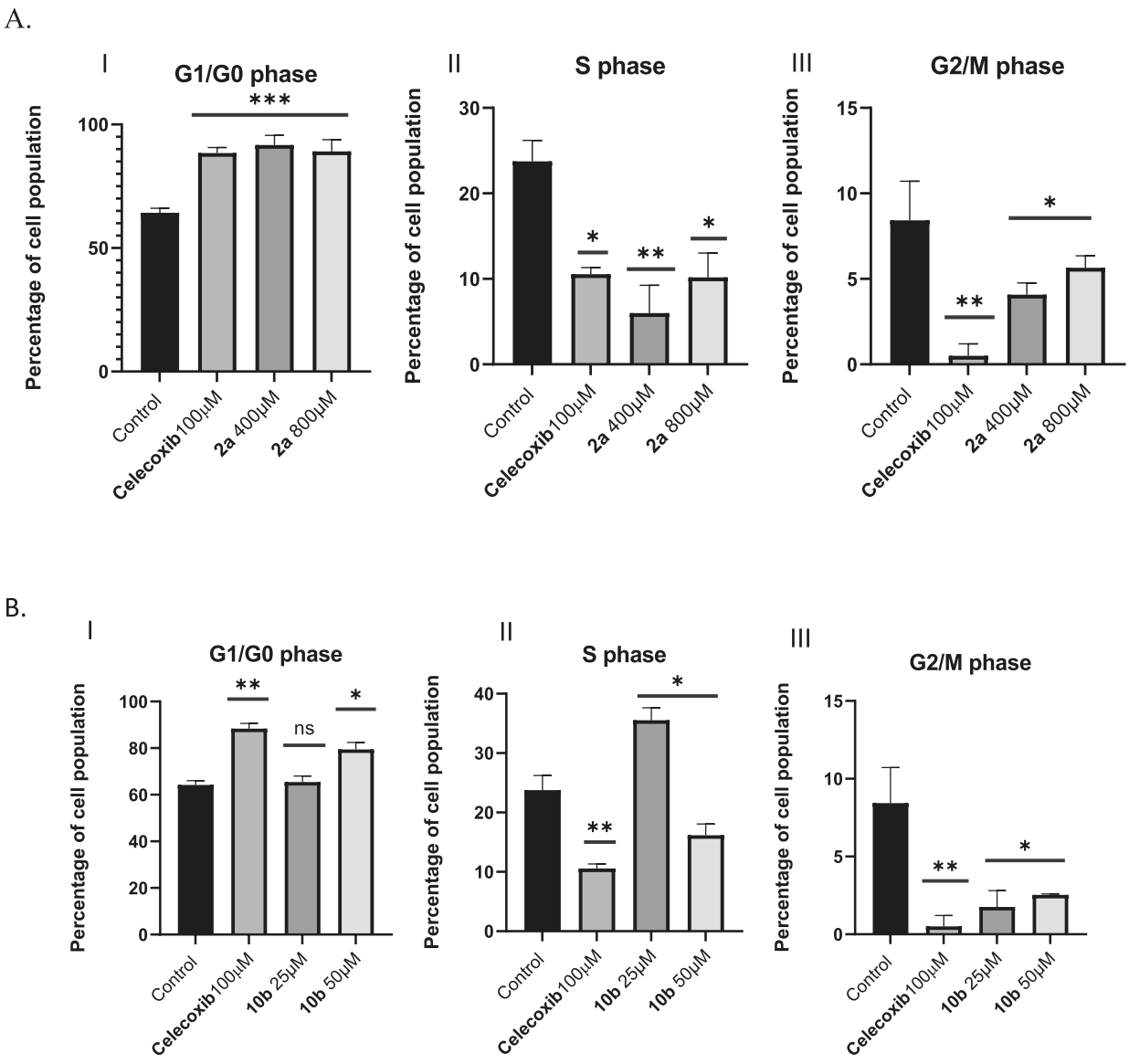

Figure 6. Effects of Celecoxib and 2a (A) and 10b (B) on Hep-G2 cell cycle progression for 24 h treatment. Data from two independent experiments performed in duplicate. Statistic bars show mean plus standard deviation; Statistic calculation was performed via Ordinary One-way ANOVA compare with control group, *P < 0.0332; **P < 0.0021; ***P < 0.0002; ****P < 0.0001, ns = not statistically significant).

(502.1 mg, 1.837 mmol), NaH (146 mg, 3.66 mmol), MeI (0.34 mL, 5.49 mmol) in DMF (0.2 M, 9.0 mL). After workup and purification on silica gel column chromatography (30% Et_2O/Hexanes, $R_f = 0.6$), desired product 3a was obtained as a pale-beige solid (417.4 mg, 79% yield). ^{1}H NMR (500 MHz, $CDCl_3$) δ 7.65 (d, $J = 8.7$ Hz, 1H), 6.96 (d, $J = 3.2$ Hz, 1H), 6.86 (d, $J = 8.7$ Hz, 1H), 6.47 (d, $J = 3.2$ Hz, 1H), 4.80 (q, $J = 8.5$ Hz, 2H), 3.92 (s, 3H), 3.69 (s, 3H). ^{13}C NMR (126 MHz, $CDCl_3$) δ 166.4, 153.8, 132.9, 130.4, 124.8, 123.8, 123.0 (q, $J_{C\text{-}F} = 277.0$ Hz), 105.4, 104.7, 101.3, 60.9 (q, $J_{C\text{-}F} = 36.6$ Hz), 57.3, 34.7. HRMS (ESI) *m/z*: $[M + H]^+$ Calcd for $C_{13}H_{12}F_3NO_3$ 288.0842, found 288.0842.

2,2,2-Trifluoroethyl 6-methoxy-1-methyl-3-phenyl-1*H*-indole-7-carboxylate (3b). Prepared by following the general procedure using indole 2b (53.0 mg, 0.151 mmol), NaH (11.5 mg, 0.286 mmol), MeI (0.02 mL, 0.286 mmol) in DMF (0.2 M, 1.0 mL). After workup and purification on preparative thin layer chromatography (20% Et_2O/Hexanes, $R_f = 0.55$), desired product 3b was obtained as a white solid (48.5 mg, 88% yield). ^{1}H NMR (500 MHz, $CDCl_3$) δ 7.92 (d, $J = 8.9$ Hz, 1H), 7.61 – 7.56 (m, 2H), 7.50 – 7.41 (m, 2H), 7.33 – 7.27 (m, 1H), 7.09 (s, 1H), 6.90 (d, $J = 8.9$ Hz, 1H), 4.81 (q, $J = 8.5$ Hz, 2H), 3.92 (s, 3H), 3.72 (s, 3H). ^{13}C NMR (126 MHz, $CDCl_3$) δ 166.3, 154.0, 134.8, 133.7, 128.8, 128.0, 127.5, 126.1, 123.0 (q, $J_{C\text{-}F} = 277.0$ Hz), 122.9, 122.6, 117.0, 105.7, 104.8, 61.0 (q, $J_{C\text{-}F} = 36.8$ Hz), 57.3, 34.8. HRMS (ESI) *m/z*: $[M + H]^+$ Calcd for $C_{19}H_{16}F_3NO_3$ 364.1155, found 364.1154.

2,2,2-Trifluoroethyl 3-ethyl-6-methoxy-1-methyl-1*H*-indole-7-carboxylate (3c). Prepared by following the general procedure using indole 2c (40.8 mg, 0.135 mmol), NaH (10.6 mg, 0.266 mmol), MeI (0.02 mL, 0.398 mmol) in DMF (0.2 M, 0.7 mL). After workup and purification on preparative thin layer chromatography (20% Et_2O/Hexanes, $R_f = 0.5$), desired product 3c was obtained as a white solid (35.0 mg, 82% yield). ^{1}H NMR (500 MHz, $CDCl_3$) δ 7.58 (d, $J = 8.7$ Hz, 1H), 6.81 (d, $J = 8.9$ Hz, 1H), 6.70 (t, $J = 1.1$ Hz, 1H), 4.77 (q, $J = 8.5$ Hz, 2H), 3.89 (s, 3H), 3.61 (s, 3H), 2.72 (qd, $J = 7.6$, 1.1 Hz, 2H), 1.29 (t, $J = 7.5$ Hz, 3H). ^{13}C NMR (126 MHz, $CDCl_3$) δ 166.4, 153.9, 133.3, 126.9, 124.3, 124.1, 121.8, 117.4, 104.5 (d, $J = 7.3$ Hz), 60.9 (q, $J_{C\text{-}F} = 36.3$ Hz), 57.4, 34.4, 17.9, 14.5. HRMS (ESI) *m/z*: $[M + H]^+$ Calcd for $C_{15}H_{16}F_3NO_3$ 316.1155, found 316.1154.

6-Methoxy-1-methyl-*N*-(2,2,2-trifluoroethyl)-1*H*-indole-7-

carboxamide (3d). To a solution of 3a (707 mg, 2.46 mmol) in 2,2,2-Trifluoro-Ethanol/Water (2:1 ratio, 0.5 M, 5.0 mL), LiOH monohydrate (775.0 mg, 6 equiv.) was added and the mixture was brought to reflux. Upon consumption of the starting material (16 h), the reaction mixture was cooled to 0 °C and 3 M HCl was slowly added until the solution reached a pH of approximately 2, as indicated by a pH indicator paper. The mixture was extracted with EtOAc (4 × 5 mL), dried over $MgSO_4$ and the solvent was removed under pressure to afford crude carboxylic acid 4 (408 mg).

To a solution of 4 (100 mg, 0.487 mmol) in DMF (0.75 M, 0.65 mL), EDC (112.1 mg, 0.584 mmol), HOBt (1.3 mg, 0.63 mmol) and DIEA (0.3 mL, 1.4 mmol) were added, followed by the addition of 2,2,2-Trifluoroethylamine hydrochloride (79.3 mg, 0.585 mmol). After stirring the reaction at room temperature overnight (16 h), 7 mL of water were added, and the mixture was acidified to a pH of 4 by addition of 3 M HCl. The mixture was extracted with EtOAc (3 × 5 mL), washed with saturated $NaHCO_3$, water, brine, and dried over $NaSO_4$, filtered through a celite plug and the organic solvents were removed under reduced pressure. The crude reaction mixture was purified by silica-gel column chromatography (20 % Et_2O/hexanes, Rf = 0.2) to afford compound 3d as a white solid (60 mg, 35 % yield over 2 steps). ^{1}H NMR (500 MHz, $CDCl_3$) δ 7.59 (d, J = 8.7 Hz, 1H), 6.93 (d, J = 3.2 Hz, 1H), 6.80 (d, J = 8.7 Hz, 1H), 6.46 – 6.37 (m, 2H), 4.18 (qd, J = 9.2, 6.6 Hz, 2H), 3.87 (s, 3H), 3.71 (s, 3H). ^{13}C NMR (126 MHz, $CDCl_3$) δ 167.3, 152.7, 133.5, 130.8, 125.1, 124.2 (q, $J_{C\text{-}F}$ = 278.8 Hz), 123.2, 108.4, 105.0, 100.9, 57.1, 41.0 (q, $J_{C\text{-}F}$ = 34.5 Hz), 35.1. HRMS (ESI) m/z: $[M + H]^+$ Calcd for $C_{13}H_{13}F_3N_2O_2$ 287.1002, found 287.1000.

6-Methoxy-1-methyl-7-((2,2,2-trifluoroethoxy)carbonyl)-1*H*-indole-3-carboxylic acid (6). To a solution of 3a (102 mg, 0.355 mmol) in DMF (0.7 mL, 0.5 M), trifluoroacetic anhydride (0.12 mL, 0.870 mmol) was added drop wise. Upon completion (monitored through TLC analysis), the reaction mixture was diluted with 3 mL of EtOAc, washed with water (3 × 2 mL), dried over $MgSO_4$ and filtered through a celite plug. The crude mixture was concentrated under reduced pressure to afford crude 5 (125.2 mg) which was used without any further purification.

To a solution of trifluoroketone 5 (100 mg, 0.261 mmol) in wet DMF (0.1 mL), NaH (31.3 mg, 0.783 mmol, 60% in mineral oil) was added and let it stir at room temperature. Upon completion, the mixture was quenched with addition of water, diluted in Et_2O and extracted with 1 M NaOH (3 × 2 mL). The combined organic layers were acidified with 3 M HCl to pH ~ 1–2 (indicated by pH paper), and extracted with EtOAc (4 × 5 mL). The organic extract was then dried with $MgSO_4$, filtered through a celite plug and concentrated under vacuum. The residue was purified by preparative TLC (50 % EtOAc/Hexanes, Rf = 0.3) to afford carboxylic acid 6 as a white solid (77.8 mg, 83% yield over 2 steps). ^{1}H NMR (500 MHz, Acetone) δ 8.26 (d, J = 8.9 Hz, 1H), 7.93 (s, 1H), 7.15 (d, J = 8.9 Hz, 1H), 5.05 (q, J = 8.9 Hz, 2H), 3.93 (s, 3H), 3.82 (s, 3H). ^{13}C NMR (126 MHz, Acetone) δ 165.3, 164.9, 154.1, 137.4, 133.4, 124.1, 123.6 (q, $J_{C\text{-}F}$ = 276.6 Hz), 122.7, 107.4, 106.6, 105.8, 60.7 (q, $J_{C\text{-}F}$ = 35.9 Hz), 56.7, 34.6. HRMS (ESI) m/z: $[M - H]^-$ Calcd for $C_{14}H_{12}F_3NO_5$ 330.0594, found 330.0593. Retention time = 28.2 min.

2,2,2-Trifluoroethyl 6-methoxy-1-methyl-3-(phenylcarbamoyl)-1*H*-indole-7-carboxylate (7). To a solution of carboxylic acid 4 (73.2 mg, 0.221 mmol) in dry DCM (0.5 M, 0.45 mL), catalytic DMF was added (2 drops). The mixture was cooled to 0°C with a water–ice bath and oxalyl chloride (0.02 mL, 0.272 mmol) was added drop-wise. After 15 min 0 °C, the ice-bath was removed and the reaction mixture was allowed to warm to room temperature and stir for additional 3 h. The reaction mixture was concentrated under reduced pressure and fresh DCM (0.45 mL) was added. The mixture was cooled to 0 °C and phenylamine (0.02 mL, 0.238 mmol) and triethylamine (0.04 mL, 0.272 mmol) were added. The reaction was monitored by TLC and, upon completion, concentrated under vacuum. The crude material was purified by silica-gel column chromatography (30% EtOAC/Hexanes, rf = 0.3), to afford amide 7 as a white solid (57.1 mg, 62% yield). ^{1}H NMR (500 MHz, $CDCl_3$) δ 8.19 (d, J = 8.9 Hz, 1H), 7.86 (s, 1H), 7.68 – 7.57 (m, 2H), 7.47 (s, 1H), 7.37 – 7.30 (m, 2H), 7.10 (tt, J = 7.3, 1.1 Hz, 1H), 6.91 (d, J = 9.0 Hz, 1H), 4.78 (q, J = 8.5 Hz, 2H), 3.87 (s, 3H), 3.57 (s, 3H). ^{13}C NMR (126 MHz, $CDCl_3$) δ 165.8, 162.8, 154.4, 138.3, 133.5, 132.5, 129.0, 124.2, 124.0, 122.9 (q, $J_{C\text{-}F}$ = 277.5 Hz), 122.0, 120.1, 110.9, 107.1, 105.0, 61.0 (q, $J_{C\text{-}F}$ = 36.6 Hz), 57.0, 35.1. HRMS (ESI) m/z: $[M + H]^+$ Calcd for $C_{20}H_{17}F_3N_2O_4$ 407.1213; Found 407.1212. Retention time = 32.4 min.

2,2,2-Trifluoroethyl 3-benzyl-6-methoxy-1-methyl-1*H*-indole-7-carboxylate (8). Following an adapted literature procedure,[29] Et_3SiH (0.13 mL, 0.46 mmol) and TFA (0.03 mL, 0.423 mmol) were added to a dry round-bottom flask, followed by the addition of toluene (0.6 M, 0.5 mL). To that solution were added benzaldehyde (0.03 mL, 0.310 mmol) followed by 3a (73.1 mg, 0.254 mmol). The mixture was heated to 50°C and was let to stir overnight (16 h). Upon completion, the reaction mixture was quenched with saturated aqueous $NaHCO_3$, extracted with DCM (3 × 2 mL), dried over $MgSO_4$, filtered through a celite plug and concentrated under vacuum. The crude was purified by silica-gel column chromatography (10 % Et_2O/hexanes, rf = 0.52 in 30% Et_2O/Hexanes) to afford compound 8 as a white solid (41.9 mg, 44 % yield). ^{1}H NMR (500 MHz, $CDCl_3$) ^{1}H NMR (500 MHz, $CDCl_3$) δ 7.50 (d, J = 8.7 Hz, 1H), 7.34 – 7.29 (m, 3H), 7.27 – 7.19 (m, 2H), 6.80 (d, J = 8.7 Hz, 1H), 6.68 (s, 1H), 4.80 (q, J = 8.5 Hz, 2H), 4.07 (s, 2H), 3.90 (s, 3H), 3.63 (s, 3H). ^{13}C NMR (126 MHz, $CDCl_3$) δ 166.4, 153.9, 140.9, 133.4, 128.7, 128.6, 128.3, 126.0, 124.3, 123.0 (q, $J_{C\text{-}F}$ = 277.5 Hz), 122.1, 114.3, 104.8, 104.6, 60.9 (q, $J_{C\text{-}F}$ = 36.6 Hz), 57.3, 34.5, 31.2. HRMS (ESI) m/z: $[M + H]^+$ Calcd for $C_{20}H_{18}F_3NO_3$ 378.1311, found 378.1311.

General Procedure for the Synthesis of 9a-9b.

To an ice-cold solution of DMF (1 M), phosphoryl chloride (3 equiv.) was added and the reaction mixture is stirred for 30 min. A solution of the corresponding indole in DMF (1.0 M) is then added and the reaction mixture is warmed up to 35ºC and stirred for an additional 1 h. After removing the reaction mixture from the heat, crushed ice is added to the flask, followed by addition of 1.0 M NaOH to neutralize the reaction mixture. After boiling the solution for 10 min, the corresponding aldehydes (9a-9c) precipitated out, and could be isolated either by filtration or by extraction with EtOAc followed by column chromatography.

2,2,2-Trifluoroethyl 3-formyl-6-hydroxy-1-methyl-1*H*-indole-7-carboxylate (9a). Prepared by following the general procedure using indole 2a (104 mg, 0.380 mmol), $POCl_3$ (0.1 mL, 1.1 mmol) and DMF (0.4 mL, 1 M). Upon filtration and purification on silica gel column chromatography (20% EtOAc/Hexanes, R_f = 0.17), aldehyde 9a was obtained as a light-brown solid (93.0 mg, 81 % yield). ^{1}H NMR (500 MHz, $CDCl_3$) δ 10.00 – 9.92 (m, 2H), 8.47 (d, J = 8.7 Hz, 1H), 7.57 (s, 1H), 6.99 (d, J = 8.9 Hz, 1H), 4.83 (q, J = 8.4 Hz, 2H), 3.86 (s, 3H). ^{13}C NMR (126 MHz, $CDCl_3$) δ 184.5, 167.1, 160.7, 140.8, 135.3, 130.4, 122.8 (q, $J_{C\text{-}F}$ = 277.5 Hz), 120.3, 118.6, 113.9, 97.8, 61.1 (q, $J_{C\text{-}F}$ = 37.2 Hz), 38.9. HRMS (ESI) m/z: $[M + H]^+$ Calcd for $C_{13}H_{10}F_3NO_4$ 302.0635, found 302.0633.

2,2,2-Trifluoroethyl 3-formyl-6-methoxy-1-methyl-1*H*-indole-7-carboxylate (9b). Prepared by following the general procedure using indole 3a (105 mg, 0.366 mmol), $POCl_3$ (0.1 mL, 1.09 mmol) and DMF (0.4 mL, 1 M). Upon filtration and purification on silica gel column chromatography (20% EtOAc/*H*exanes, R_f = 0.17), aldehyde 9b was obtained as a light-brown solid (83.0 mg, 72 % yield). ^{1}H NMR (500 MHz, $CDCl_3$) δ 9.93 (s, 1H), 8.34 (d, J = 8.9 Hz, 1H), 7.56 (s, 1H), 7.00 (d, J = 8.9 Hz, 1H), 4.79 (q, J = 8.4 Hz, 2H), 3.90 (s, 3H), 3.74 (s, 3H). ^{13}C NMR (126 MHz, $CDCl_3$) δ 184.2, 165.5, 155.1, 140.9, 134.3, 125.2, 122.9 (q, $J_{C\text{-}F}$ = 277.5 Hz), 120.7, 117.8, 108.0, 105.3, 61.1 (q, $J_{C\text{-}F}$ = 36.8 Hz), 57.0, 35.7. HRMS (ESI) m/z: $[M + H]^+$ Calcd for $C_{14}H_{12}F_3NO_4$ 316.0791, found 316.0790.

2,2,2-Trifluoroethyl 6-hydroxy-3-(hydroxymethyl)-1-methyl-1*H*-indole-7-carboxylate (10a). To a −78 °C solution of 9a (46.0 mg, 0.152 mmol) in THF (0.1 M, 2 mL), a 1 M super-hydride solution in THF was added drop wise (0.4 mL, 0.33 mmol). After 30 min, the reaction was quenched with water and extracted with a 30% Isopropanol/DCM solution (2 × 5 mL). Purification on preparative thin layer

chromatography (30% EtOAc/Hexanes, $R_f = 0.12$) afforded the desired product 10a as a clear oil (7.0 mg, 15% yield). ^{1}H NMR (500 MHz, $CDCl_3$) δ 10.10 (s, 1H), 7.83 (d, $J = 8.7$ Hz, 1H), 6.94 (s, 1H), 6.83 (d, $J = 8.5$ Hz, 1H), 4.84 – 4.77 (m, 4H), 3.74 (s, 3H). ^{13}C NMR (126 MHz, $CDCl_3$) δ 167.7, 160.3, 134.7, 129.3, 128.0, 122.9 (q, $J = 277.0$ Hz), 122.5, 116.4, 110.6, 97.1, 60.9 (q, $J_{C\text{-}F} = 36.8$ Hz), 56.7, 37.9 (d, $J_{C\text{-}F} = 1.8$ Hz). HRMS (ESI) *m/z*: $[M + H]^+$ Calcd for $C_{13}H_{12}F_3NO_4$ 302.0645, found 302.0647.

2,2,2-Trifluoroethyl 3-(hydroxymethyl)-6-methoxy-1-methyl-1*H*-indole-7-carboxylate (10b). To a −78 °C solution of 9b (83.0 mg, 0.263 mmol) in THF (0.1 M, 2.6 mL), a 1 M super-hydride solution in THF was added drop wise (0.34 mL, 1.3 equiv.). After 30 min, the reaction was quenched with water and extracted with a 30% Isopropanol/DCM solution (2 × 5 mL). Purification on preparative thin layer chromatography (30% EtOAc/Hexanes, $R_f = 0.23$) afforded the desired product 10b as a white solid (26.6 mg, 32% yield). ^{1}H NMR (500 MHz, $CDCl_3$) δ 7.73 (d, $J = 8.9$ Hz, 1H), 6.94 (d, $J = 0.9$ Hz, 1H), 6.87 (d, $J = 8.9$ Hz, 1H), 4.82 – 4.74 (m, 4H), 3.90 (s, 3H), 3.64 (s, 3H). ^{13}C NMR (126 MHz, $CDCl_3$) δ 166.2, 154.2, 133.6, 129.1, 122.8 (q, $J_{C\text{-}F} = 139.9$ Hz), 122.2, 114.9, 105.4, 104.8, 60.9 (q, $J_{C\text{-}F} = 36.6$ Hz), 57.3, 56.9, 34.6. HRMS (ESI) *m/z*: $[M - H_20 + H]^+$ Calcd for $C_{14}H_{14}F_3NO_4$ 300.0842, found 300.0841. Retention time = 28.2 min.

3-(Hydroxymethyl)-6-methoxy-1-methyl-N-(2,2,2-trifluoroethyl)-1*H*-indole-7-carboxamide (10c). Indole 9c was prepared by following the general procedure using indole 3d (51.0 mg, 0.178 mmol), $POCl_3$ (0.05 mL, 0.521 mmol) and DMF (0.2 mL, 1 M). Upon completion, the reaction mixture was extracted with EtOAc (3 × 3 mL), washed with water (5 × 2 mL), dried over $MgSO_4$ and filtered through celite to afford crude 9c (69.7 mg, 0.222 mmol).

To a −78 °C solution of crude 9c (30 mg) in THF (0.05 M, 2 mL), a 1 M super-hydride solution in THF was added drop wise (0.21 mL, 2.2 equiv.). After 30 min, the reaction was quenched with water and extracted with a 30% Isopropanol/DCM solution (2 × 5 mL). Purification on preparative thin layer chromatography (20–30% EtOAc/Hexanes, $R_f = 0.15$ in 30% EtOAc/Hexanes) afforded the desired product 10c as a white solid (16.2 mg, 67% yield over two steps). ^{1}H NMR (500 MHz, $CDCl_3$) δ 7.69 (d, $J = 8.7$ Hz, 1H), 6.92 (s, 1H), 6.83 (d, $J = 8.7$ Hz, 1H), 6.43 (t, $J = 6.7$ Hz, 1H), 4.79 (s, 2H), 4.18 (qd, $J = 9.2$, 6.7 Hz, 2H), 3.88 (s, 3H), 3.67 (s, 3H). ^{13}C NMR (126 MHz, $CDCl_3$) δ 167.1, 153.1, 134.1, 129.5, 124.2 (q, $J_{C\text{-}F} = 278.4$ Hz), 123.7, 121.7, 114.6, 108.5, 105.1, 57.1, 56.9, 41.0 (q, $J_{C\text{-}F} = 34.7$ Hz), 35.0. HRMS (ESI) *m/z*: $[M + H]^+$ Calcd for $C_{14}H_{15}F_3N_2O_3$ 316.1029, found 316.1028. Retention time = 24.0 min.

bis(2,2,2-Trifluoroethyl) 3,3′-methylenebis(6-methoxy-1-methyl-1*H*-indole-7-carboxylate) (11a). To a −78 °C solution of 9b (30 mg, 0.096 mmol) in THF (0.1 M, 1.0 mL), a 1 M super-hydride solution in THF was added drop wise (0.2 mL, 2.0 equiv.). After 30 min, the reaction was quenched with saturated NH_4Cl solution and extracted with a 30% Isopropanol/DCM solution (2 × 5 mL). Purification on preparative thin layer chromatography (20% EtOAc/Hexanes, $R_f = 0.53$) afforded the desired product 11a as a white solid (3.6 mg, 13% yield). ^{1}H NMR (500 MHz, $CDCl_3$) δ 7.56 (d, $J = 8.7$ Hz, 2H), 6.80 (d, $J = 8.7$ Hz, 2H), 6.64 (s, 2H), 4.77 (q, $J = 8.5$ Hz, 4H), 4.10 (s, 2H), 3.89 (s, 6H), 3.58 (s, 6H). ^{13}C NMR (126 MHz, $CDCl_3$) δ 166.4, 153.9, 133.4, 128.5, 124.3, 123.0 (q, $J_{C\text{-}F} = 277.9$ Hz), 122.1, 114.0, 104.7, 104.6, 60.9 (q, $J_{C\text{-}F} = 36.8$ Hz), 57.3, 34.5, 20.5. HRMS (ESI) *m/z*: $[M + H]^+$ Calcd for $C_{27}H_{24}F_6N_2O_6$ 587.1611, found 587.1612. Retention time = 29.8 min.

3,3′-Methylenebis(6-methoxy-1-methyl-*N*-(2,2,2-trifluoroethyl)-1*H*-indole-7-carboxamide) (11b). To a −78 °C solution of crude 9c (30.1 mg, 0.096 mmol) in THF (0.05 M, 2 mL), a 1 M super-hydride solution in THF was added drop wise (0.21 mL, 2.2 equiv.). After 30 min, the reaction was quenched with saturated NH_4Cl solution and extracted with a 30% Isopropanol/DCM solution (2 × 5 mL). Purification on preparative thin layer chromatography (20% EtOAc/Hexanes, $R_f = 0.28$ in 30% EtOAc/Hexanes) afforded the desired product 11b as a white solid (6.5 mg, 10% yield over two steps). ^{1}H NMR (500 MHz, $CDCl_3$) δ 7.52 (d, $J = 8.7$ Hz, 2H), 6.76 (d, $J = 8.7$ Hz, 2H), 6.65 (s, 2H), 6.37 (t, $J = 6.7$ Hz, 2H), 4.18 (qd, $J = 9.2$, 6.6 Hz, 4H), 4.09 (s, 2H), 3.87 (s, 6H), 3.63 (s, 6H). ^{13}C NMR (126 MHz, $CDCl_3$) δ 167.4, 152.8, 133.9, 128.9, 124.6, 124.2 (d, $J_{C\text{-}F} = 280.9$ Hz), 121.6, 113.7, 108.2, 104.3, 57.1, 53.4, 41.0 (d, $J_{C\text{-}F} = 34.5$ Hz), 34.8, 20.6. HRMS (ESI) *m/z*: $[M + H]^+$ Calcd for $C_{27}H_{26}F_6N_4O_4$ 585.1931, found 585.1932. Retention time = 31.1 min.

2,2,2-Trifluoroethyl 7-hydroxy-1-methyl-1*H*-indole-6-carboxylate (14). Following a reported literature procedure,[10] to a flame-dried flask equipped with a magnetic stir, $Cu(hacac)_2$ (10 mol%) is added followed by dry DCM (0.1 M), ethyl vinyl ether (10 equiv.) and diazo 1a. After attaching a reflux condenser and bringing the reaction mixture to a boil, the rection was stirred overnight (16 h). The solvent was then removed under pressure and the crude silica dispersion is purified on silica gel supported column chromatography to afford dihydrofuran acetal 13.

To a solution of $Sc(OTf)_3$ (9.2 mg, 0.019 mmol) in dry yoluene (0.9 mL, 2 M), a solution of 13 (59.9 mg, 0.188 mmol) in dry Toluene (0.9 mL, 2 M) was added and the mixture was warmed up to 70°C. Upon completion (30 min), the reaction was quenched by addition of water (2 mL), extracted with ethyl ether (3 × 4 mL), dried over $MgSO_4$ and filtered through a celite plug. The crude mixture was concentrated under vacuum purified using a silica-gel column chromatography (5% Ethyl Ether/Hexanes, $R_f = 0.63$ in 30% Ethyl Ether/Hexanes), to afford 14 as a white solid (9.5 mg, 18 % yield). ^{1}H NMR (500 MHz, $CDCl_3$) δ 11.18 (s, 1H), 7.48 (d, $J = 8.5$ Hz, 1H), 7.10 (d, $J = 2.9$ Hz, 1H), 7.07 (d, $J = 8.5$ Hz, 1H), 6.41 (d, $J = 3.1$ Hz, 1H), 4.72 (q, $J = 8.4$ Hz, 2H), 4.14 (s, 3H). ^{13}C NMR (126 MHz, $CDCl_3$) δ 169.9, 152.5, 135.8, 133.4, 124.5, 123.0 (q, $J_{C\text{-}F} = 277.5$ Hz), 119.8, 112.4, 102.1, 60.4 (q, $J_{C\text{-}F} = 37.0$ Hz), 36.6. HRMS (ESI) *m/z*: $[M + H]^+$ Calcd for $C_{12}H_{10}F_3NO_3$ 274.0685, found 274.0686.

4.2. Biological assays

4.2.1. Materials

Cell lines, including Hep-G2, A549, MDA-MB-231, MCF-7, Hela and VERO, were purchased from ATCC (Manassas, VA). $LnCaP^{F876L}$ was a generous gift from Professor John Norris, Duke University (Durham, NC). Briefly, MDA-MB-231, VERO, and A549 cell lines were maintained in Dulbecco's Modified Eagle Medium (DMEM) (Corning, 10-017-CV), supplemented with 10% fetal bovine serum (FBS) (Corning, 35-010-CV). Hep-G2, DU145, and Hela cells were cultured in phenol red free Minimum Essential Medium (MEM) (Corning, 17-305-CV), supplemented with 10% fetal bovine serum (FBS) and 2 mM Glutamine. MCF-7 cells were cultured with phenol red free DMEM (Corning 17-205-CV) with 10% FBS and 2 mM Glutamine. $LnCaP^{F876L}$ were cultured with RPMI-1640 (VWR 392-0430) with 10 %FBS and 2 mM Glutamine. CellTiter 96 Aqueous One Solution Cell Proliferation assay (MTS) kit was purchased from Promega (G3581). The COX inhibition kits (Cat. 701050) and PGE_2 ELISA kit (Cat. 500141) was purchased from Cayman. For Western blot, cleaved caspase-3, caspase-3 anti-bodies were purchased from Cell Signaling (5A1E/9662), Bcl-2 (sc-7382), Bcl-xL (sc-8392), Bax (sc-7480) and AR (sc-7305) anti-bodies were purchased from Santa Cruz. Actin was purchased from Sigma-Aldrich (A2066-100UL). Secondary antibodies – anti-mouse conjugated to IRDye680, and goat anti-rabbit conjugated to IRDye800 – were obtained from LI-COR Biosciences, Lincoln, NE. The turbo transfer kit for Midi membrane was purchased from Biorad (Cat. 1704273). Furthermore, the RNase A (RNASEA-RO) and Propidium iodide (P4170-25MG) for flow cytometry were purchased from Aldrich Sigma.

4.2.2. Cell culture and MTS assay

Hep-G2 and DU145 Cells were cultured in 10-cm petri dish with MEM medium, while VERO, A549, and MDA-MB-231 were culture with DMEM, $LnCaP^{F876L}$ in RPMI-1640 and MCF-7 were cultured in phenol red free DMEM. All the medium contains 10% FBS. For treatment, on day 1, cells were trypsinized and seeded into 96-well plates (2000 to 4500counts/well). On day 2, the cells were treated with DMSO, or 1%

DMSO solution of drugs in media such that the concentration ranges from 2.5 to 500 μM for 72 h prior to the cell viability assay. Every drug was analyzed in triplicates in the 96-well plates. Cell viability was measured using Cell MTS assay provided by Promega. Briefly, after the addition of 20 μL reagent per well, plates were incubated for 2.5–3 h at 37 °C. Colorimetric analysis was performed by measuring the signal at 490 nm. Data was analyzed according to the manufacturer's protocol. Eight data points were averaged per concentration per cell line.

4.2.3. COX inhibition colorimetric assay kit

The assay kit from Cayman (Cat. 701050) was purchased and tested for COX inhibition activities from the candidates. Following manufacturer protocol, we performed COX-1 and COX-2 inhibition assays in 5.8% DMSO solution of selected candidates in the working buffer. In brief, every candidate was diluted into 5 or 50 μM solutions incubating with recombinant COX-1 or COX-2 enzyme proteins and Hemin in reaction buffer for 5 min. Then added were 20 μL of COX Colorimetric and 20 μL COX enzymatic substrate Arachidonic acid into the plate with 2 min incubation. The plate was subsequently scanned with plate reader at wavelength of 560 nm.

4.2.4. Intracellular validation of COX inhibition

Hela cells ($1*10^6$/well) were cultured into the 6-well plates with 2 mL medium MEM and 10% FBS. The cells were seeded for 48 h prior to drug treatment. 1 mL of 0.1% DMSO or DMSO solution of Celecoxib at 10 μM, Indomethacin at 1 μM, or 10b, 10c, 2a, 2e, and 3a at 50 and 100 μM concentrations. Cells were treated for 24 h and the medium was collected into 1.5 mL Eppendorf tubes and centrifuged for 15–20 min with 13*1000 rpm. The cell debris was removed, and the supernatants (50 μL) were incubated with 50 μL PGE_2 antibody and 50 μL tracer (indicated in the manufacture instruction) in the mouse antibody coated 96-well plate. Standard, blanks, and negative controls were also incubated for 18 h with coverage. In the next day, we removed the solutions and washed wells with provided wash buffer for 5 times. The detection buffer (Ellman's reagent) was added to each well and the plate was covered with aluminum foil. The plate was incubated with shaking for 75 min. The absorbance was read in the plate reader at wavelength 415 nm.

4.2.5. Western blot

Western blotting was performed following previously published protocol.[30] In brief, Hep-G2 cells ($1*10^6$/well) were cultured in the 6-well plate and incubated for 48 h prior to the treatment. The cells were treated by DMSO (control), or 0.1% DMSO solution of 75 μM Celecoxib, 10 μM and 20 μM of compound 10b, 200 μM and 400 μM of 2a for 20 h. The cells were washed with 1X PBS before lysis with RIPA buffer (120 μLVWR, VWRVN653-100ML). The lysates were diluted to make equal protein concentration and 20–40 μg of each lysate was loaded to each well of the TGX MIDI 4–20% gel (Biorad, cat. 5671093) and ran at 150 V for 65 min. The gel was electro-blotted on to the Turbo PDVF membrane (Bio-rad, 1704273). After blocking with 5% BSA for 1–2 h, the PDVF membrane was incubated with clv-caspase, pro-caspase, Bcl-xL, Bcl-2, Bax, and Actin antibodies. After incubation overnight, the membrane was washed with TBST (3 × 5 min). Secondary antibody was added, and the membrane was incubated with agitation for 1 h. Bands were quantified using the Odyssey CLx Image system.

4.2.6. Flow cytometry

Cytometry study was performed as previously reported.[30] Hep-G2 cells were cultured until 70% confluence in a 10-cm petri dish. Cells were treated with 10 mL of 0.1% DMSO medium (control), 0.1% DMSO solution of 125 μM, 250 μM, 400 μM, and 800 μM of 2a, or 100 μM of compound Celecoxib, 12.5 μM, 25, 50 and 100 μM of compound 10b for 24 or 48 h. The medium from the wells was collected into multiple 1.5 mL centrifuge tubes and labeled. Then, cells were trypsinized and collected using cell culture medium and combined with the medium in the centrifuge tube. Then the tubes are centrifuged with RPM of 4000 for 8 min. The cell pallets were washed by 1x PBS andfixed overnight at − 20 °C using 70% ethanol. Subsequently, cells were centrifuged and washed again in 1x PBS. The suspension was treated with 200 μg/mL RNaseA for 30 min, followed by treatment with 100 μg/mL PI staining solution at room temperature for another 30 min. Cell cycle was analyzed with a BD FACS Aria-Illu Analyzer and the data processed using FlowJo.

Declaration of Competing Interest

The authors declare that they have no known competing financial interests or personal relationships that could have appeared to influence the work reported in this paper.

Acknowledgements

This work was financially supported by the National Science Foundation CHE-2102472 (S.F.) and by Georgia Tech through the Leddy Family Fellowship (S.F.); and Vasser-Woolley Fellowship and SoCB One-Time Grant (A.K.O.).

Supporting Information Available.

Autodock docking scores, full Western gels; and ^1H NMR and ^{13}C NMR spectral information. This material is available online at doi:.

Appendix A. Supplementary material

Supplementary data to this article can be found online at https://doi.org/10.1016/j.bmc.2022.116633.

References

[1] Guha R. On exploring structure–activity relationships. In: *In silico models for drug discovery*. 2013:81–94.
[2] Kaushik NK, Kaushik N, Attri P, et al. Biomedical importance of indoles. *Molecules*. 2013;18(6):6620–6662.
[3] de Sa Alves FR, Barreiro EJ, Manssour Fraga CA. From nature to drug discovery: the indole scaffold as a 'privileged structure'. *Mini Rev Med Chem.* 2009;9(7):782–793.
[4] Bhat MA, Al-Omar MA, Raish M, et al. Indole derivatives as cyclooxygenase inhibitors: synthesis, biological evaluation and docking studies. *Molecules*. 2018;23(6).
[5] Estevao MS, Carvalho LC, Freitas M, et al. Indole based cyclooxygenase inhibitors: synthesis, biological evaluation, docking and NMR screening. *Eur J Med Chem.* 2012;54:823–833.
[6] Penning TD, Talley JJ, Bertenshaw SR, et al. Synthesis and biological evaluation of the 1,5-diarylpyrazole class of cyclooxygenase-2 inhibitors: identification of 4-[5-(4-methylphenyl)-3-(trifluoromethyl)-1H-pyrazol-1-yl]benze nesulfonamide (SC-58635, celecoxib). *J Med Chem.* 1997;40(9):1347–1365.
[7] Swiatek P, Strzelecka M, Urniaz R, et al. Synthesis, COX-1/2 inhibition activities and molecular docking study of isothiazolopyridine derivatives. *Bioorg Med Chem.* 2017;25(1):316–326.
[8] Laube M, Gassner C, Kniess T, Pietzsch J. Synthesis and cyclooxygenase inhibition of sulfonamide-substituted (dihydro)pyrrolo[3,2,1-hi]indoles and their potential prodrugs. *Molecules*. 2019;24(20).
[9] Raji I, Yadudu F, Janeira E, et al. Bifunctional conjugates with potent inhibitory activity towards cyclooxygenase and histone deacetylase. *Bioorg Med Chem*. 2017;25(3):1202–1218.
[10] Guerra Faura G, Nguyen T, France S. Catalyst-controlled chemodivergent reactions of 2-pyrrolyl-α-diazo-β-ketoesters and enol ethers: synthesis of 1, 2-dihydrofuran acetals and highly substituted indoles. *J Org Chem.* 2021;86(15):10088–10104.
[11] Weng J-R, Tsai C-H, Kulp SK, Chen C-S. Indole-3-carbinol as a chemopreventive and anti-cancer agent. *Cancer Lett.* 2008;262(2):153–163.
[12] Greenhough A, Smartt HJ, Moore AE, et al. The COX-2/PGE 2 pathway: key roles in the hallmarks of cancer and adaptation to the tumour microenvironment. *Carcinogenesis*. 2009;30(3):377–386.
[13] Aoudjit L, Potapov A, Takano T. Prostaglandin E2 promotes cell survival of glomerular epithelial cells via the EP4 receptor. *Am J Physiol-Renal Physiol*. 2006;290(6):F1534–F1542.
[14] Hangai S, Ao T, Kimura Y, et al. PGE2 induced in and released by dying cells functions as an inhibitory DAMP. *Proc Natl Acad Sci*. 2016;113(14):3844–3849.
[15] Tai Y, Zhang L-H, Gao J-H, et al. Suppressing growth and invasion of human hepatocellular carcinoma cells by celecoxib through inhibition of cyclooxygenase-2. *Can Manage Res*. 2019;11:2831.

[16] Lu Q, Wang D-S, Chen C-S, Hu Y-D, Chen C-S. Structure-based optimization of phenylbutyrate-derived histone deacetylase inhibitors. *J Med Chem*. 2005;48(17):5530–5535.
[17] Li X-Z, Walker B, Michaelides A. Quantum nature of the hydrogen bond. *Proc Natl Acad Sci*. 2011;108(16):6369–6373.
[18] Shao D, Kan M, Qiao P, et al. Celecoxib induces apoptosis via a mitochondria-dependent pathway in the H22 mouse hepatoma cell line. *Mol Med Rep*. 2014;10(4):2093–2098.
[19] Tsutsumi S, Namba T, Tanaka K, et al. Celecoxib upregulates endoplasmic reticulum chaperones that inhibit celecoxib-induced apoptosis in human gastric cells. *Oncogene*. 2006;25(7):1018–1029.
[20] Grösch S, Tegeder I, Niederberger E, Bräutigam L, Geisslinger G. COX-2 independent induction of cell cycle arrest and apoptosis in colon cancer cells by the selective COX-2 inhibitor celecoxib. *FASEB J*. 2001;15(14):1–22.
[21] Anderton MJ, Manson MM, Verschoyle RD, et al. Pharmacokinetics and tissue disposition of indole-3-carbinol and its acid condensation products after oral administration to mice. *Clin Can Res*. 2004;10(15):5233–5241.
[22] Cheuk B, Leung P, Lo A, Wong P. Androgen control of cyclooxygenase expression in the rat epididymis. *Biol Reprod*. 2000;63(3):775–780.
[23] Yazawa T, Kawabe S, Kanno M, et al. Androgen/androgen receptor pathway regulates expression of the genes for cyclooxygenase-2 and amphiregulin in periovulatory granulosa cells. *Mol Cell Endocrinol*. 2013;369(1–2):42–51.
[24] Kashiwagi E, Shiota M, Yokomizo A, Inokuchi J, Uchiumi T, Naito S. EP2 signaling mediates suppressive effects of celecoxib on androgen receptor expression and cell proliferation in prostate cancer. *Prostate Can Prostat Dis*. 2014;17(1):10–17.
[25] Jendrossek V, Handrick R, Belka C. Celecoxib activates a novel mitochondrial apoptosis signaling pathway. *FASEB J*. 2003;17(11):1–25.
[26] Pan Y, Zhang J-S, Gazi MH, Young CY. The cyclooxygenase 2-specific nonsteroidal anti-inflammatory drugs celecoxib and nimesulide inhibit androgen receptor activity via induction of c-Jun in prostate cancer cells. *Can Epidemiol Prevent Biomark*. 2003;12(8):769–774.
[27] Huang K-H, Kuo K-L, Chen S-C, et al. Down-regulation of glucose-regulated protein (GRP) 78 potentiates cytotoxic effect of celecoxib in human urothelial carcinoma cells. *PLoS ONE*. 2012;7(3), e33615.
[28] Wu B, Payero B, Taylor S, Oyelere AK. Discovery of novel STAT3 DNA binding domain inhibitors. *Future Med Chem*. 2021;13(15).
[29] Pradhan TR, Kim HW, Park JK. Harnessing the polarizability of conjugated alkynes toward [2+ 2] cycloaddition, alkenylation, and ring expansion of indoles. *Org Lett*. 2018;20(17):5286–5290.
[30] Tapadar S, Fathi S, Wu B, et al. Liver-targeting class i selective histone deacetylase inhibitors potently suppress hepatocellular tumor growth as standalone agents. *Cancers (Basel)*. 2020;12(11).